Summer 2011

Dissolution of the chondrocyte cytoskeleton prevents mitochondrial oxidant release and cell death in injured articular cartilage

Ellen Elizabeth Sauter
University of Iowa

DISSOLUTION OF THE CHONDROCYTE CYTOSKELETON PREVENTS MITOCHONDRIAL OXIDANT RELEASE AND CELL DEATH IN INJURED ARTICULAR CARTILAGE

by

Ellen Elizabeth Sauter

A thesis submitted in partial fulfillment
of the requirements for the
Master of Science degree in Biomedical Engineering
in the Graduate College of
The University of Iowa

July 2011

Thesis Supervisor: Assistant Professor James Martin

Graduate College
The University of Iowa
Iowa City, Iowa

CERTIFICATE OF APPROVAL

MASTER'S THESIS

This is to certify that the Master's thesis of

Ellen Elizabeth Sauter

has been approved by the Examining Committee
for the thesis requirement for the Master of
Science degree in Biomedical Engineering at the July 2011
graduation.

Thesis Committee:_____
James Martin, Thesis Supervisor

_____
Tae-Hong Lim

_____
Todd McKinley

_____
Nicole Grosland

_____
Prem Ramakrishnan

ACKNOWLEDGEMENTS

From the beginning, my parents instilled in me the importance of an education, hard work, and a little fun. It is with their love, encouragement, and support that I am the person I am today. To my brother, Matt, thank you for always being there for me; you are an amazing man whom I can always looked up to. For all this and more, I thank my entire family from the bottom of my heart. To all my friends, especially Sarah, Abbie, Stephanie, Ben, Allie, Abraham, and Chloe, thanks for believing in me and keeping me sane.

I would like to thank my research advisor, Dr. James Martin for the amazing opportunity to work and learn from him and his guidance throughout my research. Dr. Todd McKinley, thanks for your counsel and enthusiasm on this project. Thanks to Dr. Prem Ramakrishnan for our many discussions. Thank you to Dr. Nicole Grosland and Dr. Tae-Hong Lim; I have enjoyed learning from you and my time at Iowa. And to the Orthopaedic Cell Biology Lab, it has been an honor to work with all of you. You have been there for me in the best and the trying times, and I appreciate everything you have done for me. I would also like to thank Lois Lembke and Theresa Messlein for their administrative assistance. You are all extraordinary people, and I will miss our dance parties. Also, I need to acknowledge the CORT NIH P50 AR055533 Grant for funding this research. Big thanks also go out to the Central Microscopy Research Facility at the University of Iowa for the use of their facilities, without which, my project would have been impossible.

I would also like to thank all my teachers from throughout my academic career and my professors from Gustavus, especially my undergraduate advisor, Dr. Colleen Jacks, my viola instructor and orchestra director, Warren Friesen, and Dr. John Lammert who inspires everyone with his passion for teaching and learning.

Once again, thanks to everyone. This has been an amazing opportunity for me to learn and grow, and I will remember this experience my entire life.

TABLE OF CONTENTS

LIST OF TABLES

Table

LIST OF FIGURES

Figure

CHAPTER 1

INTRODUCTION

Osteoarthritis, a debilitating, degenerative joint disease, is one of the leading causes of disability in the work place. It causes devastation to the synovial joints, destroying articular cartilage and other joint tissue and causing sever joint pain. Primary osteoarthritis has no identifiable initiation event and affects mostly people over the age of 45. Primary osteoarthritis has been considered an age related disease. However, secondary osteoarthritis occurs after a specific event such as intra-articular fracture, or blunt impact to the synovial joint and affects a much younger population than primary osteoarthritis, making available treatments for primary osteoarthritis, such as joint replacement, not suitable for many of those patients affected by secondary osteoarthritis. There is no cure yet for osteoarthritis and some aspects of the disease are not well understood, and many different pathways of joint degeneration have been shown to play critical roles in the etiology of the disease. Once these pathways are better understood, osteoarthritis will be able to be better treated.

The homeostasis and health of synovial joints are reliant on the responses of the joint's components to their mechanical loading environment, especially the responses of the articular cartilage.[3, 4] As the unique cell type present in articular cartilage, chondrocytes are responsible for the regulation of their metabolism and the synthesis of their surrounding matrix and modify these functions according to mechanical stimuli.[3] Chondrocytes are therefore responsible for the health of articular cartilage and the joint. Not all loading is beneficial to the articular cartilage. In fact, impact injury, abnormal loading, and overloading can lead to chondrocyte metabolic dysfunction and death, either by necrosis, premature cell death, or apoptosis, programmed cell death. The acute effects of the events following cartilage injury and chondrocyte apoptosis and necrosis play an important role in the long term progression of post-traumatic osteoarthritis (PTOA).

A cascade of biological events that can lead to osteoarthritis is triggered during overloading and impact injury to synovial joints. After injury, not only does chondrocyte death occur by necrosis and apoptosis, but the extracellular matrix (ECM) surrounding chondrocytes starts to degrade instigating the onset of osteoarthritis.[5, 6] While most chondrocyte death directly after injury is necrotic and occurs within the first 12 hours after impact,[7] chondrocyte death has also been shown to occur by apoptosis after cartilage injury and accounts for much of the later chondrocyte death. Additionally, it has been shown that the release of excessive reactive oxygen species (ROS) after a high energy impact plays a role in the initiation of chondrocyte apoptosis,[7, 8] and by treating osteochondral explants with antioxidants, in particular N-acetylcysteine (NAC) and vitamin E, Martin and colleagues were able to rescue chondrocytes after injury.[7] This rescue of chondrocytes with antioxidant treatment points to ROS as an initiator of chondrocyte death after impact. Release of ROS after impact substantially decreases 24 hours after impact which correlates to the initial chondrocyte death after injury. Goodwin et al. showed that the excessive release of ROS after cartilage injury was induced by chondrocyte mitochondria and was mitigated by treating explants with rotenone, a mitochondrial electron transport inhibitor, thereby improving chondrocyte viability after injury.[8] This evidence implies that mitochondrial dysfunction, mainly the excessive release of ROS after impact, leads to chondrocyte death which causes cartilage degradation. Understanding how mitochondrial dysfunction and ROS release leads to chondrocyte death could help to prevent the progression of injury related PTOA.

Mechanical loading and therefore mechanotransduction play a major role in the progression of PTOA. Normal, dynamic loading regulates chondrocyte metabolism and matrix production while injury whereas abnormal loading leads to the overproduction of ROS, chondrocyte death, and matrix degradation. Therefore, the structural integrity of chondrocytes and their surrounding ECM are pivotal to articular cartilage health. The cytoskeleton of chondrocytes, the microfilaments, the microtubules, and the intermediate

filaments, interact to maintain the physical structure of chondrocytes and are important to mechontransduction pathways. While the stiffness of chondrocytes are less than those of the surrounding matrix, the stiffness of chondrocytes plays a critical role in the mechanotransduction of intracellular signaling via the cytoskeleton.[9] With chondrocyte deformation, cytoskeletal elements transmit strain to intracellular organelles, including the mitochondria.[10]

Microfilaments, mainly filamentous actin, are responsible for the cell's resistance to compression and have been shown to be concentrated around the chondrocytes' periphery, facilitating the attachment of chondrocytes to the surrounding ECM.[11] Not only are microfilaments associated with the ECM, they also have attachments with chondrocyte mitochondria. Along with the microfilaments, the microtubules and intermediate filaments play roles in cell structure and cell signaling. Microtubules have been shown to co-localize with the mitochondria. With an intact cytoskeleton, mitochondria experience distortion upon chondrocyte deformation. Inhibition of microfilaments or microtubules drastically reduces the movement of mitochondria. This evidence shows that mitochondria are physically coupled to the cytoskeletal network. Thus, mitochondria are potentially subjected to external loads applied to the articular cartilage through their cytoskeletal attachments. Tissue level strains not only macroscopically deform tissues but are therefore conducted to the intracellular organelles, especially the mitochondria, via the cytoskeleton.

From this evidence, it was therefore hypothesized that with inhibition of chondrocytes' cytoskeletal elements, the release of ROS from the chondrocyte mitochondria would be repressed and chondrocyte viability after impact would increase when compared with specimens not treated with cytoskeletal inhibitors. To test this hypothesis, osteochondral explants were treated with cytoskeletal inhibitors, either cytochalasin B which in inhibits the microfilaments or nocodazole which disrupts microtubule polymerization. Explants were subjected to an injurious load and imaged

using confocal microscopy for ROS production directly after impact and viability 24 hours after injury. On analysis, cytoskeletal inhibitors were found to reduce mitochondrial ROS production directly after impact and increase chondrocyte viability at 24 hours after impact.

CHAPTER 2

BACKGROUND AND SIGNIFICANCE

2.1 Osteoarthritis

Osteoarthritis is a debilitating, degenerative joint disease caused by synovial joint degeneration (Figure 1.) It affects almost 27 million Americans, more people than any other joint disease. Often arising without any identifiable cause, osteoarthritis results in chronic joint pain and dysfunction, and in advanced stages, it can lead to joint contracture, muscle atrophy, and limb deformity. Because of the pain and loss of

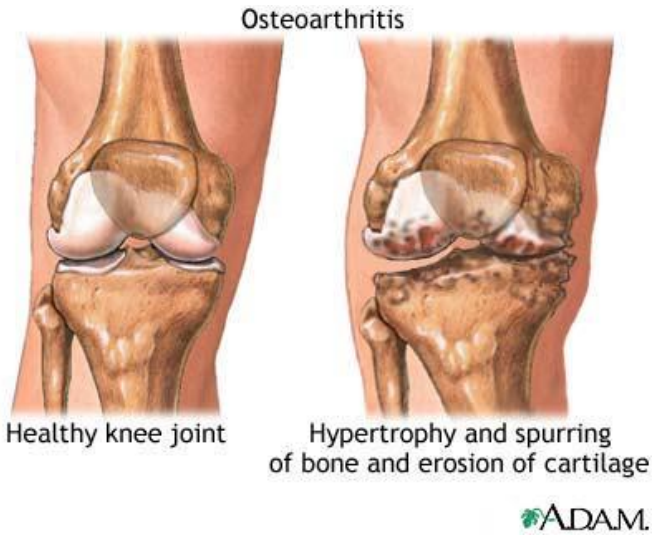

Figure 1. Comparison of normal and osteoarthritic knee anatomy. http://www.nlm.nih.gov/medlineplus/ency/imagepages/17103.htm

mobility, osteoarthritis is the leading cause of disability in the work place and is estimated by the Arthritis Foundation to cause a $124 billion/year societal financial burden, which is only expected rise as the population ages.[12] Currently, there is no cure for osteoarthritis; however, a better understanding of the pathogenesis of the disease could lead to better treatments.

There are two types of osteoarthritis, primary and secondary. Primary osteoarthritis is generally associated with aging and affects more than 10% of the population. Osteoarthritis usually develops after the age of 45[13] and most people over the age of 65 display the pathology of the disease though many do not display symptoms. Secondary osteoarthritis is usually associated with a particular event, be it injury, infection, etc., and often develops much earlier in life than primary osteoarthritis.

Post-traumatic osteoarthritis (PTOA), a secondary osteoarthritis, develops secondary to synovial joint trauma and accounts for almost 12% of the overall financial burden of osteoarthritis.[12] The outcomes of intra-articular fractures have changed little over time, with many cases progressing to PTOA.[14] Even with the best care available for joint injuries, the risk of developing PTOA ranges from 20% in the acetabulum fractures to more than 50% in distal tibia fractures involving the articular surface.[15-17] In 2005, the U.S. spent approximately $3 billion of health care costs on the 5.6 million people with symptomatic PTOA of the hip, knee, or ankle.[12]

The progression of PTOA is a result of the mechanical injury itself and also the biological events occurring after injury. However, not all the events leading to PTOA are well understood, but they do affect the entire synovial joint. Since PTOA is an organ-level disease, the pathoetiology must be understood at the organ-level for treatment of the disease to be successful. Articular fractures are not the only events that lead to the progression of PTOA; ligamentous or meniscal tears, or even capsular damage and joint dislocation can lead to PTOA. These injuries cause chondrocyte dysfunction and death and lead to ECM degradation in the articular cartilage. On average, people that suffer from PTOA are younger than those patients presenting with primary osteoarthritis by 9-14 years.[12, 18] Since most of these patients are younger than the primary osteoarthritis population, joint replacement is an unsuitable option for treatment. A better understanding of the initiation and progression of PTOA will help to develop better treatments for this debilitating disease.

2.2 Synovial Joint Anatomy

There are three categories of joints in the human body, fibrous, cartilaginous, and synovial (Figure 2). Each are described by the way and/or type of material in which the articulating bones are joined. Bones of fibrous joints are connected by fibrous tissue, and movement in these joints depends on the length of fibers present in the joint. However, most fibrous joints allow for little or no movement within the joint, such as the sutures of the cranium or teeth in the mandible and maxilla. Cartilaginous joints are those that are connected by hyaline or fibrocartilage, such as the costal cartilage of the rib cage that connect the ribs to the sternum and the intervertebral discs of the spine. These joints allow for slight bending through the joint.

Unlike fibrous or cartilaginous joints which allow little or no motion within the joint, the third type of joint, the synovial joint, allows for motion in the joint. These are the joints that permit one to move from place to place and allow one to interact with the surrounding world. However, this free motion leads to a higher incidence of joint injury.

Synovial joints can be classified into six major types by the shape of the articulating surfaces and/or the type of movement they permit (Figure 2).[19] Plane joints

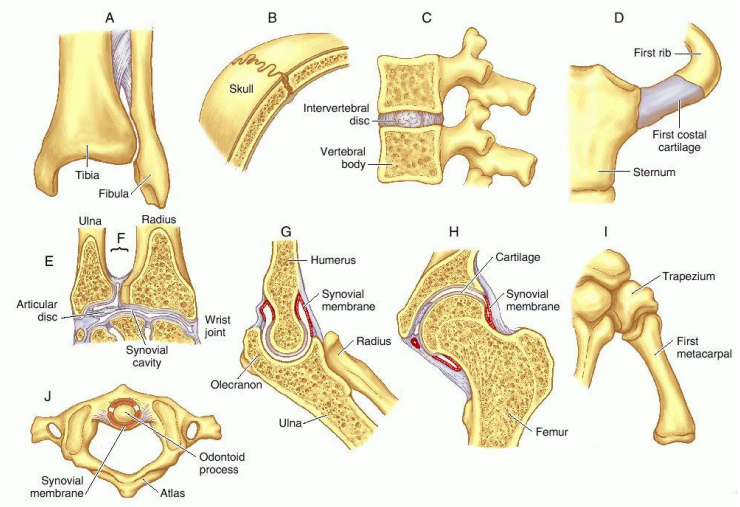

Figure 2. Joint types in the body. http://medical-dictionary.thefreedictionary.com/synovial+joint

are those that permit gliding movements in the plane of the articular surfaces, and the participating bones are usually fairly flat with a tight joint capsule. The acromioclavicular joint, between the acromion of the scapula and the clavicle is an example of a plane joint. The next type of synovial joint is the hinge joint; it only allows for flexion and extension in one plane, around a single axis. The joint capsule of hinge joints is thin and lax in the anterior and posterior directions to allow for joint flexion and extension. The bones of hinge joints are held strongly together by laterally placed collateral ligaments. The elbow and the knee are two examples of hinge joints. Saddle joints allow for adduction and abduction as well as flexion and extension of the joint. The adjoining surfaces in these joints are reciprocals of each other, one being convex, while the other is concave. The thumb is an example of a saddle joint. Condyloid joints, such as in the metacarpolphalangeal joints, are joints that permit the same movements as the saddle joint except that in one plane, the movement is greater than in the other. Ball-and-socket joints allow movement in multiple planes and axes. They are highly mobile and consist of a spheroidal surface of one bone set within the socket of another. The largest ball-and-socket joint of the human body is the hip joint, where the head of the femur articulates with the acetabulum of the pelvis. The last type of synovial joint is the pivot joint which allows for rotation around a central axis such as in the rotation of the head, facilitated by the atlas (C1 vertebra) and the axis (C2 vertebra).

Synovial joints occur at the junction of two or more articulating bones and are united by an articular capsule (Figure 3). This articular capsule is continuous with the periosteum of the bones forming the joint and consists of two layers. The outermost layer is made up of a fibrous tissue consisting of dense, irregular connective tissue, mostly collagen, and may include ligaments that help to support the structural integrity of the joint. The flexibility of the articular capsule’s fibrous tissue allows for substantial movement while providing great tensile strength to the joint, preventing the dislocation of the articulating bones. Accessory ligaments, which help to provide tensile strength to the

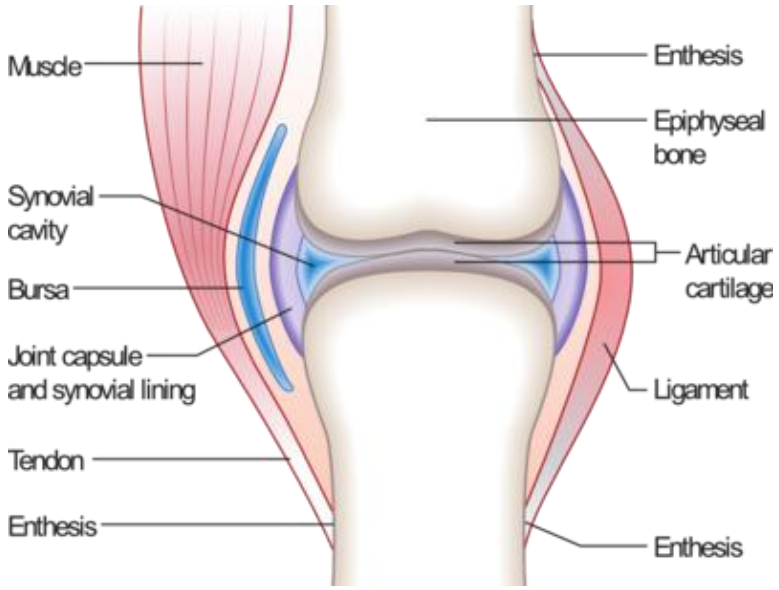

Figure 3. Schematic of a synovial joint.
http://en.wikipedia.org/wiki/Synovial_joint

joint and hold the bones close together, can either be separate from the joint capsule (extrinsic ligaments) or can be a thickening of a part of the joint capsule itself (intrinsic ligaments).

Just deep to this outer, fibrous tissue lays the synovial membrane which is composed of areolar tissue with elastic fibers and secretes synovial fluid into the joint capsule. This synovial fluid forms a thin film over all the interior surfaces of the synovial joint capsule and helps to lubricate the articular cartilage of the articulating bones. It helps to reduce friction between articulating surfaces and provides a bit of shock absorption for the joint. Since the interior of the synovial joint is avascular, synovial fluid, secreted by the synovial membrane, supplies oxygen and nutrients to the articular cartilage by way of diffusion. It also removes carbon dioxide and metabolic wastes produced by the chondrocytes of the articular cartilage.

Blood supply to synovial joints is delivered by the articular arteries which arise from vessels around the joint. The articular arteries anastomose to form networks so that blood is continually supplied to the joint no matter its position. The arteries and veins of the joint capsule are located in the synovial membrane and do not penetrate the synovial fluid or articular cartilage. Along with a rich blood supply, synovial joints have considerable nerve supply to the joint capsule. Most nerves that supply synovial joints are branches of nerves that supply the muscles that move the joint. The synovial membrane is relatively aneural, while the fibrous portion of the capsule and the associated ligaments are well innervated to respond to movement and injury. Like the vasculature of the synovial joint, the nerves of the joint do not penetrate into the joint capsule.

Menisci are also present in several different synovial joints. They are disc-like structures made of very dense fibrocartilage and are attached to the fibrous capsule. Laying between the articulating surfaces, the menisci subdivide the articular capsule, help to absorb the stresses of physiological loading, and direct flow of synovial fluid to areas in the joint that experience the greatest friction and loading. The menisci permit incongruent surfaces of articulating bones to fit more securely together, creating greater stability in the joint. A good example of this is in the knee, where two extremely incongruent surfaces meet, the rounded condyles of the femur and the fairly flat surfaces of the tibial plateaus. The menisci between these two bones help to stabilize the joint, along with the surrounding ligaments, tendons, and muscles.

Movement of synovial joints creates friction throughout the joint. In many of the large synovial joints of the body, bursae, sac-like structures, are situated at strategic sites throughout the joint to help minimize friction between soft tissues and other synovial joint structures. Although they are not technically a part of the synovial joint, the fluid-filled bursal sacs cushion the movements of the synovial joint components, such as the contacts between skin and bone, ligaments and bone, muscles and bones, and tendon and bones. Tendons that experience a lot of friction are encased by tendon sheaths to reduce

friction. Many synovial joints also include articular fat pads which are accumulations of fat tissue that also help to cushion the joint.

Articulating surfaces of synovial joint bones are covered with a layer of specialized, hyaline cartilage called articular cartilage. The main functions of the articular cartilage are to provide a smooth, low friction contact area between articulating bones and stress absorption during normal movement.[20] Progression of osteoarthritis is a result of the dysfunction and destruction of the chondrocytes and the surrounding extracellular matrix of the articular cartilage.

The health of synovial joints is dependent upon the health of all its components. If a component of the joint is not working properly, it affects the homeostasis of the entire joint. To be able to better treat osteoarthritis, a better understanding of how the disease affects the entire joint is needed.

2.3 Knee Anatomy

The knee is the largest, most superficial of the synovial joints in the human body making it one of the most susceptible joints to injury (Figure 4). It is also one of the most common joints affected by osteoarthritis. The knee allows for the extension and flexion of the lower limb, aiding in walking, and it also permits a small amount of rotation about the vertical axis of the body.

The bones that make up the knee joint are the condyles of the distal femur, the lateral and medial plateaus of the tibia, and the patella. Because of the incongruous nature of the articulating surfaces of the knee, rounded condyles sitting on the relatively flat surface of the lateral and medial tibial plateaus, the knee is a relatively weak synovial joint. Because of this weakness, the knee relies on the strength of the surrounding muscles, tendons, and ligaments connecting the femur and tibia for stability in the joint. The crescent-shaped menisci of the knee also help to stabilize the incongruent surfaces of the femur/tibia juncture.

The joint capsule of the knee consists of the usual outer fibrous layer and the inner synovial membrane. The fibrous layer consists of a few thickened parts of intrinsic ligaments but for the most part is relatively thin and even incomplete in some areas.

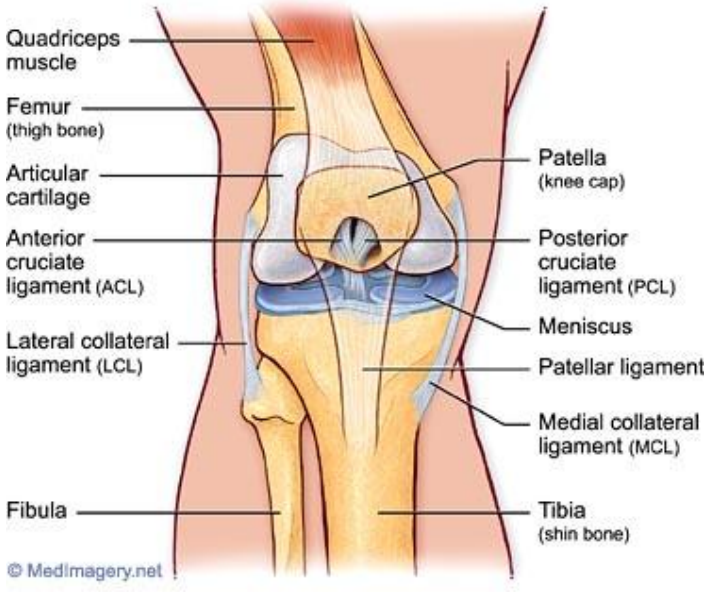

Figure 4. Anatomy of the knee joint.
http://www.orthspec.com/knee_anatomy.htm

Anteriorly, the quadriceps tendon, the patella, and the patellar ligament replace the fibrous layer of the joint capsule. The synovial membrane lines the interior surface of the entire capsule except for the articular cartilage.

The knee joint is strengthened by five extra-capsular ligaments and the intra-articular ligaments. The extra-capsular ligaments include the patellar ligament, the medial and later collateral ligaments, and the oblique and arcuate popliteal ligaments. Flexion and extension of the knee is facilitated by the patellar ligament, a strong, thick fibrous band extending from the tibial tuberosity to the apex and adjoining margins of the patella. Located medially and laterally to the femur and tibia in the knee, the medial and lateral collateral ligaments, respectively, contribute greatly to the stability of the joint in full

extension. The oblique and arcuate popliteal ligaments both help to reinforce the knee capsule posteriorly. The anterior cruciate ligament (ACL) originates at the anterior intercondylar area of the tibia while the posterior cruciate ligament arises from the posterior intercondylar area of the tibia. The cruciate ligaments of the knee crisscross within the capsule but are outside the synovial cavity. These ligaments help to maintain the close contact between the femur and the tibia. The ACL limits posterior rolling and displacement of the femoral condyles, while the PCL limits the anterior rolling and displacement of femur on the tibia.

2.4 Articular Cartilage

Articular cartilage is a specialized hyaline cartilage which covers the articulating surfaces of the bones in synovial joints. It consists of a unique cell type, the chondrocyte, in a specialized extracellular matrix (ECM) of collagens, non-collagen proteins, and proteoglycans, type II collagen and aggrecan being the most abundant of these molecules. Mechanical stimuli, biochemical factors, and genetic factors combine to regulate the metabolism and function of articular cartilage and contribute heavily to the overall health of synovial joints.

Chondrocytes, the only cell type present in healthy articular cartilage, form only 1-5% of the entire volume of the entire articular cartilage. Since there are so few chondrocytes in articular cartilage, most chondrocytes are isolated in a dense ECM with little to no cell-to-cell interactions. Even without cell-to-cell interactions, these few, specialized chondrocytes are responsible for the health of the entire articular cartilage and for the maintenance and synthesis of the ECM. They depend on the diffusion of nutrients through the dense extracellular matrix for nutrition from the synovial fluid and because of the relative impermeability of the matrix, the size of the diffusing molecules and their electrical charge significantly influence the diffusion of nutrients to the intended chondrocytes.

Collagen forms 10-20% of articular cartilage wet weight.[21] Type II collagen is the most prominent type of collagen in articular cartilage, comprising 90-95% of all collagen present. It provides tensile strength to the cartilage. In the different zones of cartilage, the collagen fibers are oriented to best suit the mechanical requirements of the specific zones of cartilage (Figure 5). In the superficial zone, collagen fibers lie parallel to the cartilage surface to provide shear strength to manage stresses caused by friction during movement. However, as collagen progresses to the deeper zones of articular cartilage, collagen fibers become more radially oriented until they are perpendicular to the cartilage surface in the

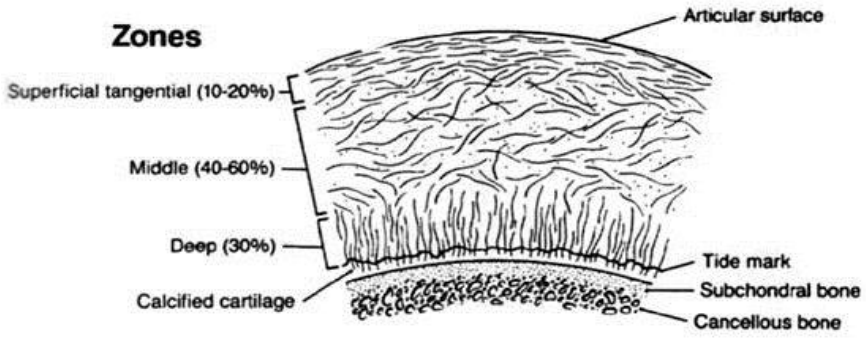

Figure 5. Collagen structure in the different zones of articular cartilage.
http://www.orthoteers.com/(S(0wprhkggw0b1vhhjn0usgz3q))/mainpage.aspx?section=29&article=137

deep zone of cartilage, giving the cartilage in this zone a more rigid structure. In the absence of deep vertical fibrils in cartilage finite element analyses, the maximum cartilage tensile/shear strains were shown to substantially increase.[22] The vertical orientation of collagen fibrils in the deep zone of cartilage plays a huge role in the stiffness of the articular cartilage and protects chondrocytes from excessive strains. However, with removal of the superficial zone collagen fibrils, there was a less significant effect on cartilage strain and stiffness.[22]

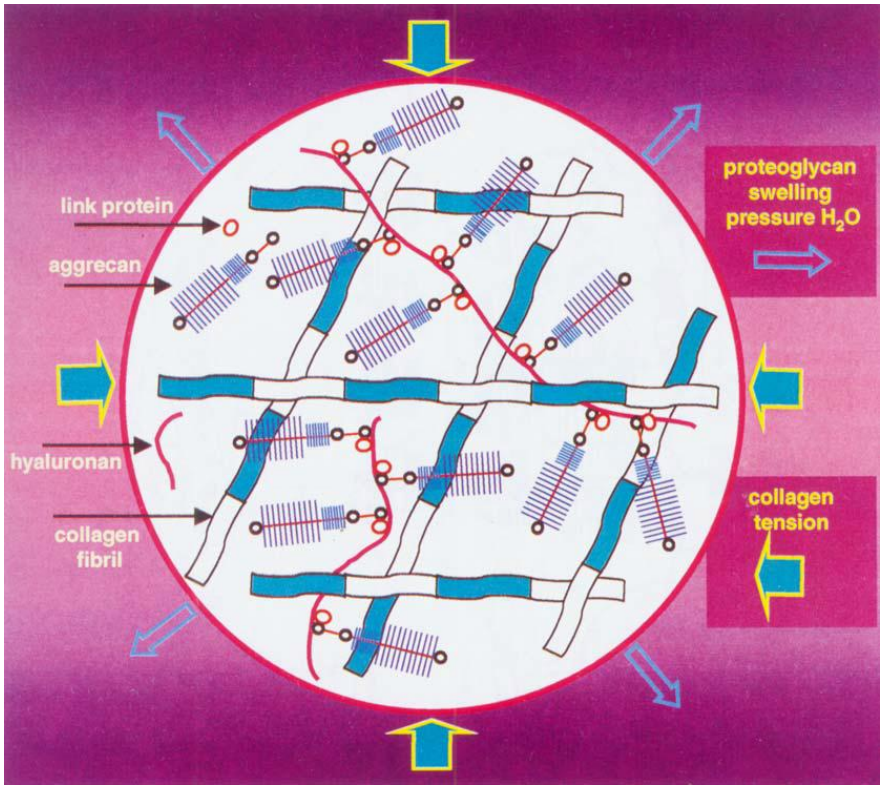

Figure 6. Properties of aggrecan and collagen in articular cartilage.[1]

Proteoglycans are proteins which provide for compressive stress in articular cartilage with a wet weight of 10-20% in articular cartilage (Figure 6).[21] Aggrecan is the major proteoglycan produced by chondrocytes in articular cartilage, and is an aggregate of glycosaminoglycan (GAG) side chains non-covalently linked to a hyaluronic acid backbone. Link protein, a small glycoprotein, helps to stabilize the connection between GAG and hyaluronic acid. About 90% of aggrecan mass is made up of the GAG side chains, which consists of mostly chondroitin sulfate and to a lesser extent keratin sulfate. Because of the negatively charged anionic groups of the GAG side chains, water is drawn into cartilage because of the osmotic imbalance created by these molecules and aggrecan's inability redistribute itself because of the bulk of its side chains.[1] The interactions of proteoglycans, collagen, and water are critical to the biomechanical

makeup of articular cartilage. The collagen network in articular cartilgae resists the expansion of aggrecans, contributing to the mechanical properties of cartilage.

Water makes up 65-80% of articular cartilage's wet weight. Most water is in the superficial zone with the amount of water decreasing deeper in the cartilage as proteoglycan content increases. Water allows for load-dependent deformation and provides nutrition and lubrication for the joint.

Articular cartilage is composed of four discrete regions: the superficial or tangential zone, the middle or transitional zone, the deep or radial, zone, and the calcified cartilage zone. Constituents of articular cartilage are uniquely organized in each of these zones.

The superficial zone, also called the tangential zone, is the thinnest of the four zones and is covered by a thin film of synovial fluid containing lubricin which is important for joint lubrication. The chondrocytes of the superficial zone lie parallel to the surface of the cartilage and have a flat, ellipsoid shape.[21] Along with these flattened chondrocytes, the collagen fibers in the superficial zone are thin and form a network of fibers that lie parallel to the articular surface and provide great tensile and shear strength to the cartilage.

The transitional zone lies just deep to the superficial zone and contains chondrocytes with a more spheroidal shape surrounded by ample ECM. Collagen fibers in this region are thicker than those in the superficial zone and are arranged in a somewhat radial fashion. Proteoglycan content is much higher in the transitional zone than in the superficial zone providing superior mechanical properties to those in the superficial zone.[21]

The spheroidal chondrocytes of the deep zone are arranged in columns perpendicular to the articular surface. In this zone, collagen fibers are the thickest and proteoglycan content is the highest.

The calcified cartilage zone is a mineralized zone lying just above the subchondral bone but beneath the tidemark. The small numbers of chondrocytes in this zone have very low metabolic activity but synthesize type X collagen, which provides structural integrity and some shock absorption along the articular cartilage-subchondral bone interface. The density of chondrocytes progressively decreases from the superficial zone to the calcified cartilage zone whereas the proteoglycan content increases, creating anisotropic mechanical properties in articular cartilage.

2.5 Mechanical Loading

The health of synovial joints relies heavily on the mechanical environment of the joint. It is a delicate balance between beneficial and detrimental loading. Radiographic evidence shows that there is no difference in the joints of long distance runners and non-runners. Former championship runners over the age of 55 were no more likely to have osteoarthritis than non-runners.[23] In fact, moderate runners have increased articular cartilage thickness, proteoglycan content, and indentation stiffness when compared with non-runners which suggests that repetitive loading is beneficial to cartilage health. However, those people who participate in sports that subject synovial joints to more severe impact and torsional loading, such as soccer, football, or basketball to name a few, are more likely to develop osteoarthritis than a normal person.[23] From these results, it is evident that frequency and magnitude of loading play a role in the progression of osteoarthritis. Along with overloading of synovial joints, prolonged immobilization of a joint can also have detrimental effects on the joint, reducing the proteoglycan content and synthesis in the articular cartilage.[24] Not only does immobilization adversely affect articular cartilage, it affects the bones, ligament metabolism, and mechanical properties.[23]

Articular cartilage is constantly subjected to varying levels of mechanical stress, be it from walking, running, writing, talking or any other movements produced by synovial joints. This dynamic mechanical environment is an extremely important component affecting the homeostasis of articular cartilage, and therefore, synovial joint

health as well. When isolated from cartilage, chondrocytes dedifferentiate into fibroblast-like cells. They fail to maintain their phenotype and are no longer able to make glycosaminoglycans, both of which are essential for cartilage health and structure.[25] These findings suggest that the native, three dimensional environment, including the ECM and mechanical loading, of chondrocytes provides cues to maintain the overall health of cartilage. It has been shown that when chondral explants are subjected to an intermittent, uniaxial load with a peak stress of 0.5MPa at 0.2Hz for 10 cycles, the proteoglycan and collagen content of the cartilage increased along with the mechanical properties of the explant.[26] Whereas dynamic loading increases glycosaminoglycan and protein synthesis, static loading impedes their synthesis.[3] Dynamic loading is more physiological than static loading, so it is reasonable that dynamic loading would enhance the properties of articular cartilage while static loading inhibit its properties.

Different zones of articular cartilage respond differently to mechanical loads because of the anisotropic nature of articular cartilage. Guilak et al. showed that local strains caused the greatest decrease in cellular height in the superficial zone chondrocytes while the transitional and deep zone chondrocytes experienced significantly less deformation.[9] Langelier et al. also found that labeling of chondrocyte cytoskeletal elements was more intense in the superficial zone of articular cartilage suggesting that these superficial zone chondrocytes develop a more robust cytoskeleton to enhance their structural function in a region of cartilage that experiences greater strains.[11] In the deeper zones of articular cartilage, chondrocytes experience less deformation than in the superficial zone and rely more on hydrostatic pressure and the collagen network for structural integrity; therefore, they do not need as dense of cytoskeleton elements as the chondrocytes of the superficial zone.[11]

It was shown that with the deformation of chondrocytes, organelles within chondrocytes also deform, including the rough endoplasmic reticulum, the Golgi apparatus and the mitochondria[27]. Szafranski et al. found that the rough endoplasmic

reticulum and mitochondria lost water in the same proportion as the nucleus and ECM upon tissue compression.[27] Therefore, any shape changes to these organelles are most likely from interactions with one or more of the components of the chondrocyte cytoskeleton, the microtubules, the microfilaments, or the intermediate filaments. The mechanical integrity of chondrocytes was compromised when chondrocytes were treated with cytoskeletal inhibitors, cytochalasin D to inhibit the microfilaments or nocodazole to inhibit the microtubules.[28] These cytoskeletal elements were shown to be essential for strain transfer to the intracellular organelles. When articular cartilage is loaded, the strain created by the load is carried through the cytoskeleton of the chondrocyte to the mitochondria, causing deformation to the mitochondria as well as to the rest of the cell.

Mechanical stress greater than the physiological range applied to a joint can adversely affect the general health of the joint, often leading to the onset of osteoarthritis. Mechanical injury to the articular surface results in the apoptosis of chondrocytes, especially in the vicinity of the injury site[29], in both human and bovine cartilage.[30, 31] Apoptosis seems to be dose related, increasing with greater applied loads,[32] and loss of chondrocyte viability after injury is accompanied by ECM degradation.[5, 31] During an injury to the cartilage, the collagen network is disrupted, releasing GAGs from the cartilage.[30] This disruption of the collagen network releases GAGs from the cartilage and also allows remaining GAGs to draw in excess water because of all the negatively charged anionic groups on the GAG chains of aggrecan, causing the tissue to swell and tissue strain to increase. Loss of glycosaminoglycans (GAGs) from articular cartilage is an indicator of damage and dysfunction of the ECM. However, GAG loss alone does not induce chondrocyte death, as shown by Otsuki et al.[33] When GAG-depleted cartilage is exposed to a mechanical injury, chondrocyte death is apparent, with much of the death being necrotic. Also, the cracks created in the cartilage during injury were much larger than in normal cartilage. It is possible that GAG depletion in cartilage increases the net

strain on the tissue and compromises the tissue's mechanical properties which may contribute to cell death during mechanical injury.

After an injurious load is applied to chondral explants, an initial rapid phase of cell death occurs, associated with chondrocyte necrosis[34], followed by a slower phase of cell death, usually apoptotic, that propagates from the injury site.[35] Tochigi et al. also found that chondrocyte death in human tibial plafond fractures was much greater at the fracture edge and radiated out from the fracture edge.[29] These findings imply that a cascade, or multiple cascades, of biological signals are given off by chondrocytes, inducing chondrocyte apoptosis after the initial injury.

Since articular cartilage is both avascular and aneural, growth of blood vessels and nerves from the subchondral bone that penetrate into the articular cartilage is an abnormal event but has been shown to be amplified in osteoarthritic and rheumatoid arthritic cartilage.[36] Normal cartilage is usually hostile to invasion by blood vessels; however, this ingrowth of vasculature and nerves aids the progression of osteoarthritis and causes joint pain.[37]

2.6 Cytoskeleton

The cytoskeleton of chondrocytes aids in the transduction of mechanical stimuli to specific regions of the cell that turn the stimuli into biological signals. Eukaryotic cells have three major structural elements, microfilaments, microtubules, and intermediate filaments. Each of these elements has their own distinct size, structure, and intracellular distribution, and is formed by the polymerization of different subunits.[38] A cell's cytoskeleton provides structural integrity for the entire cell and aids in mechanotransduction of cell signaling. The components of the cytoskeleton are structurally and functionally linked together. Cells use the cytoskeletal network to create a tensegrity architecture to control their shape and structure. In the tensegrity model, components of the cytoskeleton stabilize themselves through the use of tensile prestresses.[39] This network is composed of tensed elements, microfilaments, and

elements that resist being compressed, microtubules. The tensed elements tend to pull toward the center of the cell while the others resist compression, resulting in a state of isometric tension that makes the cytoskeleton strong and responsive to external mechanical stresses.

Microfilaments of articular cartilage are the greatest contributor to the bulk cell stiffness, while microtubules and intermediate filaments play a central role in cellular volumetric changes and compressibility.[40] Ofek et al. also showed that microtubules exerted the greatest influence on cell recovery from an applied compressive force and were aided by the microfilaments and intermediate filaments. Disrupting the tensegrity architecture of the cell using cytoskeletal inhibitors specific to a certain cytoskeletal element affects all the components of the cytoskeleton, not just the element targeted by the inhibitor. An example of this is when microfilaments in a cell are depolymerized; the depolymerization of the microfilaments alters the distribution of microtubules and microtubule-associated organelles not just the microfilaments.[41] However, these effects are minimal on the untargeted cytoskeletal elements when compared to the targeted elements.[40] The cytoskeletal elements are connected to external structures of the ECM through focal adhesions and serve as an intracellular transportation vehicles.

Microtubules are the largest of the cytoskeletal elements (Figure 7). They are hollow cylinders made up of α-tubulin and β-tubulin polypeptides with an outer diameter of about 25nm and an inner diameter of about 15nm. Microtubules have many functions including the maintenance of cell shape. Formation of mitotic and meiotic spindle fibers used in the movement of chromosomes during cell division is a function of the microtubules, and they are involved in the distribution and movement of vesicles and organelles within the cell, including the mitochondria. Microtubules resist bending and twisting when force is applied, and are formed by the addition of α- and β-tubulin dimers which are oriented in the same direction, giving microtubules a distinct polarity. Addition of tubulin dimers occurs more readily at the plus end of the microtubule. In chondrocytes,

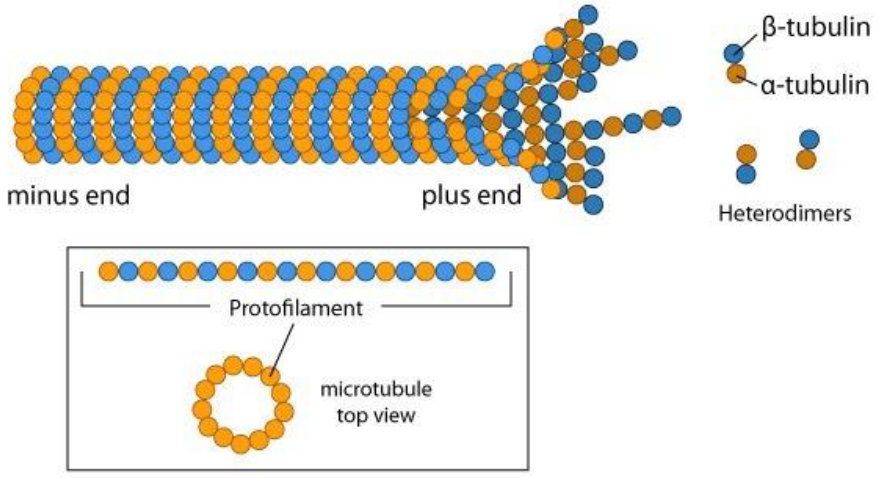

Figure 7. Structure of microtubules. http://manual.blueprint.org/Home/glossary-of-terms/mechano-glossary--m/mechano-glossary-microtubules

microtubules from a loose, basket-like mesh throughout the cytoplasm suggesting that microtubules are stabilizing elements in chondrocytes and help transport materials throughout the cell.[11] The interaction of the Golgi apparatus with the cell's microtubules facilitates proteoglycan synthesis which is essential for cartilage health by responding to dynamic stresses on the tissue.[42, 43] Mitochondria have also been shown to partly co-localize with microtubules suggesting an association between the structures.[10]

Nocodazole is an antimitotic agent that blocks microtubule assembly by binding to β-tubulin, preventing the formation of one of the two interchain disulfide bonds. Binding of nocodazole to β-tubulin at the polymerization site prevents further microtubule assembly. The inhibition of the microtubule network by colchicine, which produces a similar effect as nocodazole, was shown to block the redistribution of mitochondria in the maturation of human oocytes demonstrating that mitochondria in cells are linked to and distributed by the microtubule network.[44] In the distribution of mitochondria around the cell by the cytoskeleton, mitochondria inherently must be subjected to some level of strain. Since mitochondria are associated with the microtubule network of the cell, the depolymerization of microtubules could block the transfer of

injurious strains to the mitochondria, obstructing the release of reactive oxygen species (ROS) upon impact or overloading of the articular cartilage. Consequently, blocking ROS production could lead to increased chondrocyte viability after impact and cartilage health.

Microfilaments have a diameter of about seven nanometers, making them the smallest of the cytoskeletal structural elements. Most notably, microfilaments are known for their role in the contractile fibers of muscle cells. However, microfilaments also play an important role in cell movement, division, and maintenance of cell shape. Globular actin, G-actin, monomers reversibly polymerize to form microfilaments. Two strands of G-actin wind together into a helix to form filamentous actin, f-actin (Figure 8). Like

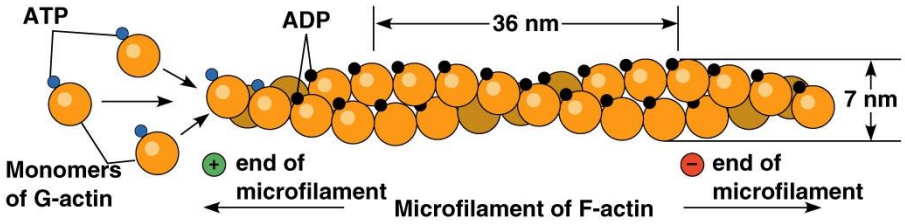

Figure 8. Structure of the microfilament f-actin. http://virtual.yosemite.cc.ca.us/rdroual/Lecture%20Notes/Unit%201/Cytology%20with%20figures.htm

microtubules, microfilaments form polar molecules which polymerize more readily at the plus end, or barbed end of the molecule. Cells actively regulate the assembly of microfilaments which contribute greatly to the bulk cell stiffness of articular cartilage chondrocytes.[40, 45] In chondrocytes, dense and punctate actin is found at the peripheral cortex, helps to protect against damaging shear strain, and is important in maintaining chondrocyte phenotype.[11] Localization of actin filaments with viniculin at the cell membrane suggests that the actin cytoskeleton forms focal adhesions to the ECM providing a link for transmission of mechanical stresses and strains.[46] Cartilage responds

to varying mechanical stimuli; therefore, the stiffness of the cartilage and chondrocytes plays a major role in the transmission of biological signals in articular cartilage.

Cytochoalasin B is a fungal metabolite that interferes with the polymerization of actin in cells. It also inhibits the glucose transport system in some cell membranes.[47] Cytochalasin B impedes actin polymerization by slowing the rate of monomer addition at the barbed end of the growing filament but does not significantly alter filament assembly at the pointed end.[47, 48] However, filament growth at the pointed end is at least six times slower than polymerization at the barbed end.[49] The slowed polymerization of f-actin inhibits the formation of the chondrocyte cytoskeleton; therefore, the connection between the f-actin and mitochondria is compromised. Because this connection is compromised, impact strain cannot be transmitted to the mitochondria which in turn reduce the amount of ROS produced during injurious loading, and chondrocytes experience an increase in viability when compared to injured chondrocytes with intact cytoskeletons.

Having a diameter of about 8-12nm, intermediate filaments are the middle-sized elements, as well as the most stable of the cytoskeletal constituents. Intermediate filaments are specific to tissue type. In the case of chondrocytes, vimentin is the most prominent of the intermediate filaments. Vimentin intermediate filaments form a tighter, finer mesh that traverses chondrocytes' cytoplasm.[11] In chondrocytes, vimentin disassembles and reassembles in response to mechanical stimuli and may be involved in mechanical signal transduction.[11]

2.7 Mitochondria

Mitochondria are often called the "energy powerhouse" of the cell and are believed to have bacterial origins. Typically, the major role of the mitochondria is to produce ATP for cellular metabolism. However, in chondrocytes, cell metabolism is minimal, and in osteoarthritic cartilage, mitochondrial functioning is further altered. Irregular functioning may be a result of mitochondrial DNA mutations or the direct effects of cytokines, prostaglandins, or even ROS of the electron transport chain (Figure

9). It has been shown that pro-inflammatory cytokines interleukin-1β (IL-1β) and tumor necrosis factor-α (TNF-α) induce mitochondrial DNA damage which plays a crucial role in the proper functioning of mitochondria and consequently chondrocytes. This damage is also an initiating factor in the increase of mitochondrial ROS production following cytokine treatment.[50] The majority of this ROS production originates with the electron transport chain of the mitochondria. The electron transport chain uses the transfer of electrons through a series of complexes that are coupled to the translocation of protons across the mitochondrial inner membrane, creating a proton gradient which in turn

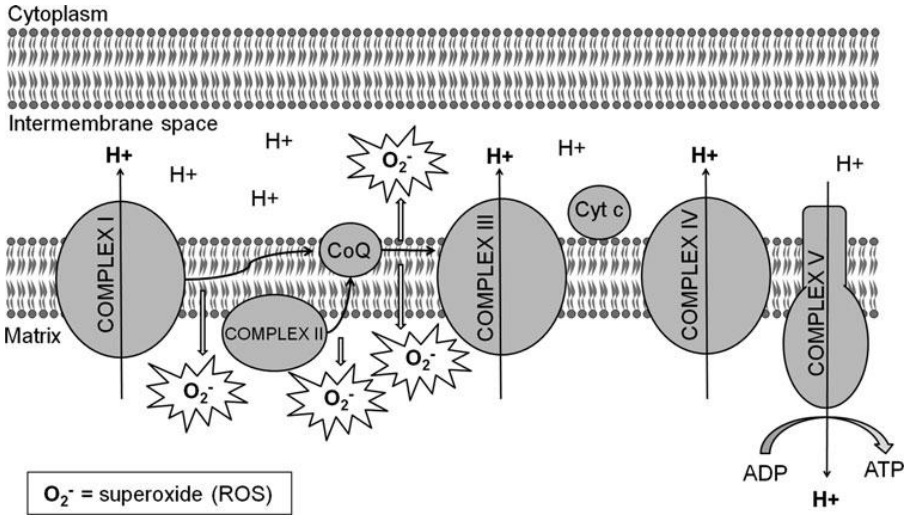

Figure 9. Electron transport chain in mitochondria.[2]

generates ATP for cellular functioning. During the transfer of electrons from one complex to another, especially from complex I to ubiquinone and from ubiquinone to complex III, some electrons escape and react with oxygen to form reactive oxygen species.[2] It has been shown that the activity of complexes I, II, and III are all decreased in osteoarthritic chondrocytes.[13]

In response to an applied force, mitochondria experience significant deformation and displacement. However, when cytoskeletal elements are inhibited by drugs that

prevent the polymerization of these elements, the motion and deformation of mitochondria is drastically decreased indicating a close association of mitochondria with the chondrocyte's cytoskeletal elements.[51] Actin microfilaments are a vital component of mitochondrial-specific transport system.[52] Knight et al. showed that upon chondrocyte deformation, mitochondria experience distortion which could indicate that they may play a role in mechanotransduction of cellular signals.[10] Ali et al. showed that cyclic strain induced an increase in mitochondrial ROS signaling in endothelial cells.[53] Together with Knight et al.'s work, these results point to a mitochondrial role in a mechanotransduction pathway leading to the release of ROS from mitochondria. In support of these findings, Goodwin et al. found that when bovine osteochondral explants were subjected to an injurious load and treated with rotenone, an agent that impedes the release of ROS from mitochondria by binding to the ubiquinol binding site of the mitochondrial respiratory chain's complex I, thereby blocking the flow of electrons to complex III, ROS release was reduced.[8]

2.8 Reactive Oxygen Species Production

Reactive oxygen species have been implicated in many different diseases such as cardiovascular diseases, types of cancer, type two diabetes mellitus, and even Alzheimer's disease, to name a few.[13] However, that is not to say that all ROS are detrimental to cells' general health, and in some cases, they are essential for homeostasis. Being an avascular tissue, articular cartilage is adapted to functioning in very low oxygen conditions when compared with most other tissues. Because of its low oxygen environment, cartilage relies heavily on glycolysis for ATP production and to carry out normal metabolic functions. Lee and Urban found that although chondrocytes under anoxic conditions remained viable for many days, the sulfate incorporation and lactate production stayed low[54] showing that matrix maintenance and metabolism were impeded. With the addition of oxygen or other types of oxidants, sulfate incorporation and lactate production rose substantially.[54] These findings indicate that articular cartilage requires

oxidants to stimulate glycolysis for energy production and to maintain chondrocyte metabolism and ECM synthesis. Conversely, Ysart and Mason showed that though very high oxygen tensions in bovine chondrocytes stimulate glycosaminoglycans in the short term, ultimately, GAG synthesis is inhibited showing that too much oxygen can be harmful for articular cartilage.[55] Also, glycolysis rates were highest in chondrocytes under low oxygen conditions and glucose uptake and lactate production were both high at those levels of oxygen. The level of oxygen present in articular cartilage plays a critical role in the homeostasis of the tissue.

Chen et al. have shown that the chondrocytes of osteoarthritic cartilage in porcine knee joints have higher levels of oxidative DNA damage. The more oxidative DNA damage present, the higher the Mankin score, which measures the severity of osteoarthritic lesions, the higher the Mankin score, the greater the severity of osteoarthritis. Because of this oxidative damage, DNA transcription errors may occur which could lead to abnormal protein production and matrix degradation.

Intracellular ROS regulate a large number of intracellular signaling pathways including those involved in cell growth and differentiation. They also act as intermediates for cytokines and growth factors.[56] Vascular endothelial growth factor (VEGF) promotes degradation pathways in articular cartilage as well as ROS. Fay et al. determined that the 60-fold difference of VEGF present in synovial joint fluid of patients with osteoarthritis as opposed to those with healthy joints was caused by the presence of ROS or the activation of the production of O_2 in the cartilage.[57]

Chondrocytes are adapted to carry out the necessary processes for cartilage homeostasis in a hypoxic environment and an increase of oxygen in this environment could be detrimental to articular cartilage. Oxygen tensions in cartilage range from almost 10% at the cartilage surface to less than one percent in the deep and calcified cartilage zones.[58] It is possible that disruption of the articular surface through injury exposes cartilage in deeper regions to greater oxygen tensions not usually seen by those

chondrocytes. This excessive exposure to oxygen may damage chondrocytes throughout the injury site and elicit the progression of cartilage degeneration through different processes.

A number of studies have shown that there is an association between mechanical stress and an escalation of ROS production.[8, 53] This increase in ROS production results in ECM degeneration and chondrocyte apoptosis in articular cartilage. One study shows that when human cartilage explants were treated with antioxidants such as n-acetyl-cysteine (NAC), superoxide dismutase (SOD), catalase, or vitamin E prior to cyclic loading, chondrocyte viability was significantly higher than those explants that were cyclically loaded without an antioxidant treatment indicating, that ROS production is a significant factor in chondrocyte apoptosis.[59] Taken together with the fact that antioxidants also had an anti-apoptotic effect on explants, these results indicate that oxidative damage plays a role in chondrocyte apoptosis. After injury to the articular surface, ROS is released from chondrocytes.[8] Martin et al. showed that not only does N-acetyl-cysteine preserve chondrocyte viability following impact injury, but it significantly inhibits matrix GAG loss at impact sites for up to 14 days after the original injury.[7] From this information, it seems that pathophysiologic events ascribed to ROS production occur soon after injury.

In association with the cytoskeleton and mitochondria of chondrocytes in articular cartilage, release of ROS species sets in motion the pathogenesis of PTOA. Cellular level strain is transferred to chondrocytes' mitochondria via the cytoskeleton. Upon deformation, mitochondria release excessive amounts of ROS which leads to chondrocyte death and ECM degradation.

2.9 Objectives

Osteoarthritis is a devastating synovial joint disease characterized by pain and loss of function in synovial joints brought about by the destruction of the joint and in particular the articular cartilage. Synovial joint health is dependent on the mechanical

environment of the articular cartilage which help to regulate chondrocyte metabolism and ECM synthesis by the chondrocytes. There is a balance between beneficial and detrimental loading to which chondrocytes respond respectively. Overloading and injury to the joint lead to chondrocyte death and ECM degradation through multiple pathways. One of these pathways is initiated by the excessive release of ROS from the mitochondria following injurious loading. The application of cytoskeletal inhibitors before impact could prevent the overproduction of ROS by disconnecting the mitochondria from the cytoskeleton. The inhibition of the connection between the mitochondria and the cytoskeleton would relieve the strain put on the mitochondria by the cytoskeleton during injurious loading. Therefore, if the injurious strain is not transmitted to the mitochondria, the mitochondria will not be able to release excessive amounts of ROS and chondrocyte viability increases.

CHAPTER 3

MATERIALS AND METHODS

3.1 Harvest and Culture of Osteochondral Explants

Mature bovine stifle joints were obtained after slaughter from a local abattoir (Bud's Custom Meats Inc, Riverside, IA) (Figure 10). First, muscle, synovia, and fat were dissected away from the lateral and medial portions of the stifle joint. The lateral collateral and medial collateral ligaments were then severed. This allowed for the exposure of the anterior cruciate ligament (ACL) and the posterior cruciate ligament (PCL). These two ligaments were then cut and the femur was removed. Next, the patella was removed from the tibial tuberosity by cutting through the thick patellar ligament and surrounding tissue. The lateral and medial tibial plateaus remained covered by the lateral

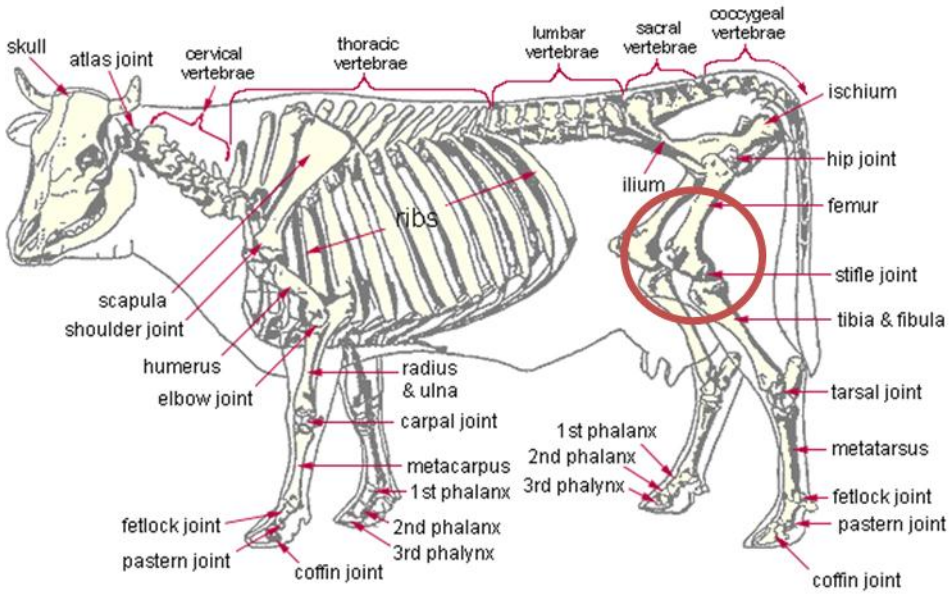

Figure 10. Bovine skeletal anatomy. The stifle joint, circled in red, is the equivalent of the human knee. Bovine stifle joints were used to examine the effects of cytoskeletal dissolution on ROS production and chondrocyte viability. http://www.backyardherds.com/forum/viewtopic.php?id=199

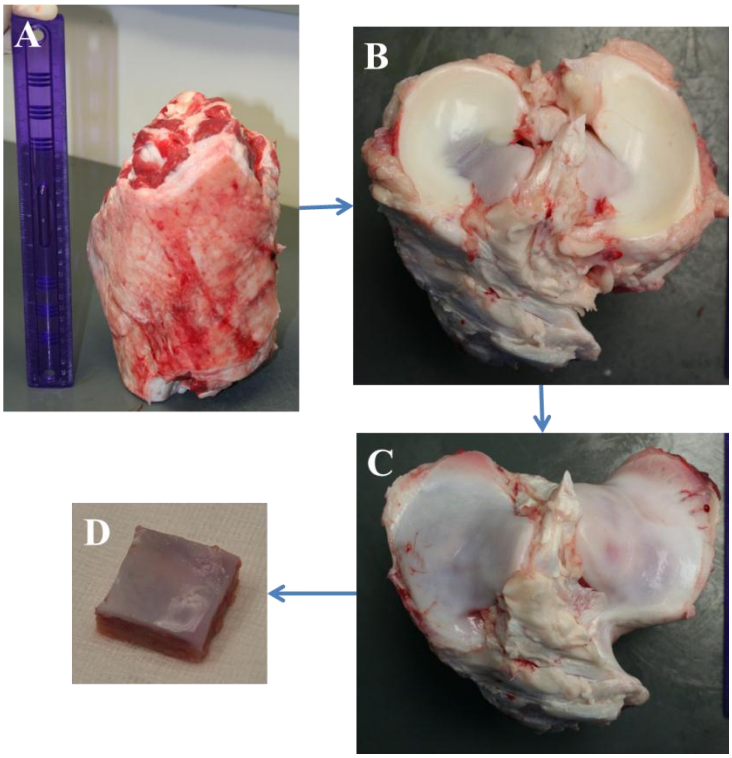

Figure 11. Dissection of the bovine stifle joint. A) Stifle joint obtained from abattoir. B) Tibial plateaus of a right stifle joint with menisci still attached. C) Tibial plateaus with menisci dissected away. D) Osteochondral explant harvested from bovine stifle joint.

and medial menisci, respectively (Figure 11). The menisci were then excised to expose the lateral and medial tibial plateaus for explant harvest (Figure 11).

Osteochondral explants, 2.5cm x 2.5cm x 1.0cm, were harvested from the portion of the lateral and tibial plateaus uncovered by the menisci using a handsaw. Specimens that were impacted were taken from lateral tibial plateaus because of their more level articulating surface for a flat impact, while medial tibial plateaus were used for f-actin staining with phalloidin (Figure 12). Explants were then placed in Hanks' Balanced Salt Solution (HBSS) containing amphotericin B (1.5µg/ml) and Pen Strep (50 units/ml penicillin and 50µg/ml streptomycin) to keep the explants from getting infected. Using a scalpel, the edges of articular cartilage of the osteochondral explants were trimmed to

reduce damage to the adjacent cartilage and were placed in HBSS containing antibacterial and antifungal agents for a second time (Figure 12).

Explants were rinsed with fresh Hanks' solution containing antibiotics and antifungal treatments and placed in culture medium containing 45% DMEM (Dulbecco Modified Eagle Medium), 45% Ham's F-12, and 10% fetal bovine serum (FBS) (Invitrogen) and incubated overnight under low oxygen conditions (5% O_2, 5% CO_2) at 37°C. The next day explants were transferred to low O_2-equilibrated Phenol Red-Free culture medium (10% FBS, 1:1 DMEM/F12 (Ham) 1x) and cultured again overnight under the same low oxygen conditions.

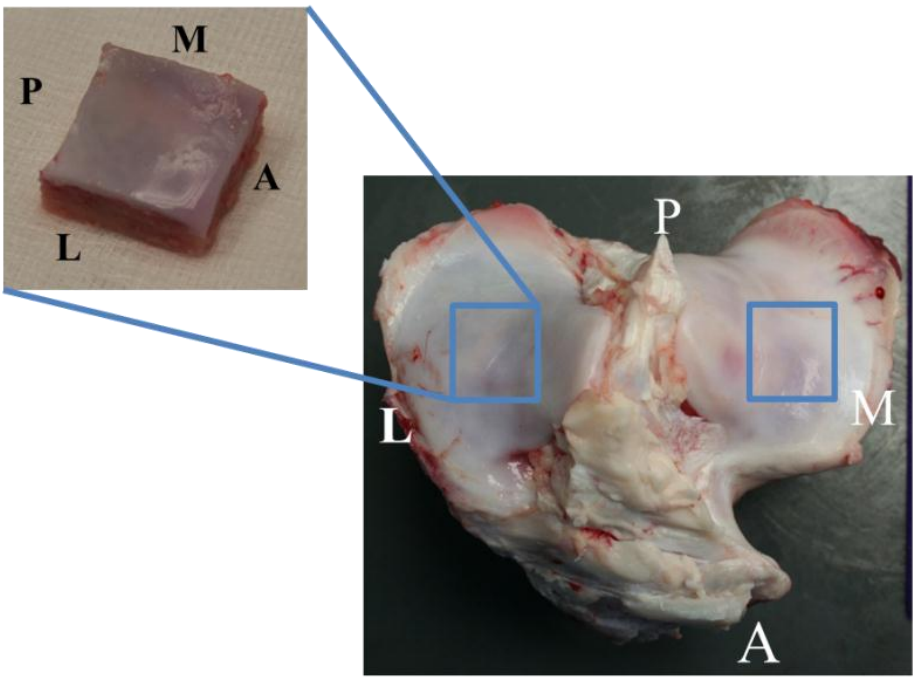

Figure 12. Harvest sites of lateral and medial osteochondral explant from a right bovine stifle joint. Boxes indicate location of harvest of osteochondral explant. L-lateral, M-medial, A-anterior, and P-posterior.

3.2 Pre-Impact Treatment

Prior to impact injury, experimental specimens were treated with 20 μM cytochalasin B (Calbiochem; n=8) or 10μM nocodazole (Sigma; n=8) for four hours in Phenol Red-Free culture medium under low O_2 conditions at 37°C. Untreated specimens (n=7) were maintained in low O_2 conditions until impact injury.

3.3 Impact of Osteochondral Explant

Osteochondral explants were fastened into a custom built impact device with four screws, one into each side of the bone of the osteochondral explant, making sure that the

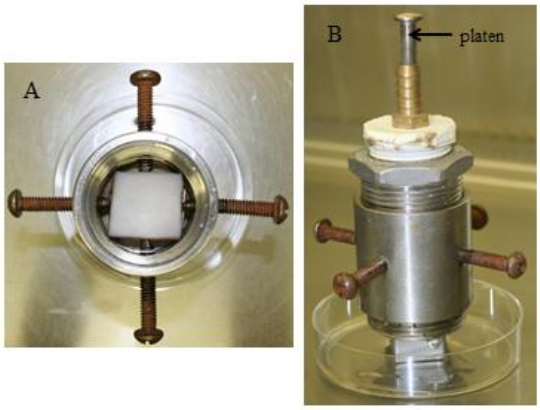

Figure 13. Osteochondral impactor chamber. A) Osteochondral explant loaded in the impactor chamber and covered with low O_2 media. B) Assembled impactor chamber with impact platen resting on top of articular cartilage.

explant was level for a flat impact surface (Figure 13). Low O_2 equilibrated culture medium covered explants at all times during impact. A 5.0-mm diameter, flat-faced brass rod with rounded edges (r=1.0-mm) was rested on top of the explant. A two-kilogram mass was dropped from a height of seven centimeters onto the brass rod to produce a 7 J/cm^2 impact to the articular surface (Figure 14). Immediately after impact, the mass was

removed from the brass rod. After removal of the mass and brass rod, explants were removed from the impact device. Pre-treated and untreated osteochondral explants were secured to a plastic plate with polycaprolactone (PCL; Aldrich) to facilitate imaging with a custom made stage driver. After impact, specimens were either probed for ROS production and imaged or placed in Phenol Red-Free culture media and incubated overnight under low O_2 conditions for viability imaging 24 hours after impact.

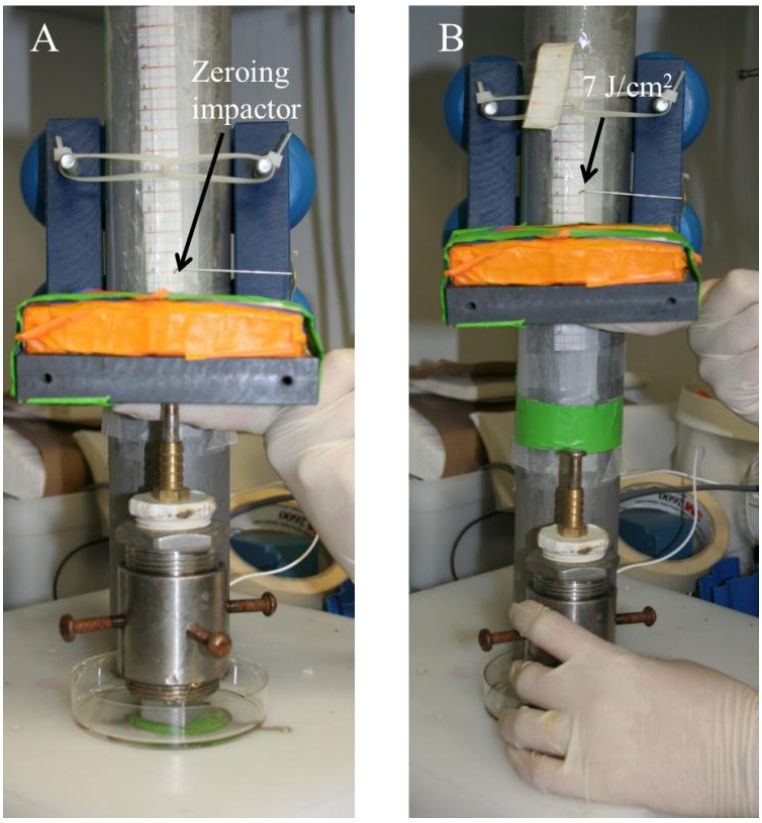

Figure 14. Impactor setup. A) Zeroing of the impact device. B) Two kilogram mass ready to impart a 7 J/cm^2 impact.

3.4 Imaging

3.4.1 Oxidant Production

To study the effects of pre-impact treatment of articular cartilage with cytoskeletal inhibitors on reactive oxygen species, ROS, production after impact, specimens were placed in Phenol Red-Free culture medium containing 5μM dihydroethidium (DHE; Invitrogen), a superoxide probe, and 1mM Calcein AM (Invitrogen), a live cell probe, for 30 minutes at the previously specified low O_2 conditions directly after impact and fixation to the plate.

Experimental specimens were imaged on a BioRad 1024 Confocal Microscope equipped with a Krypton/Argon laser. Three 20x sites within the impact zone and three 20x sites at least 0.5cm away from the impact zone were imaged for further analysis. Sites were scanned using wavelengths of 568nm and 488nm for DHE and Calcein AM, respectively. Laser power was set at 10% and the iris was set at 3.5 during imaging. The gain and offset were adjusted at each location. Each site was scanned to a depth of about 140μm at intervals of 20μm to create a z-stack. Following imaging, explants were placed in fresh, low O_2 equilibrated phenol red-free culture medium and incubated overnight at low O_2 conditions for viability imaging 24 hours after impact.

3.4.2 Viability

To analyze the effect of cytochalasin B, nocodazole, and no treatment on the viability of chondrocytes in articular cartilage 24 hours after impact, osteochondral explants were probed with Calcein AM (1mM) and ethidium homodimer-2 (EthD-2; 1mM) (Invitrogen), a dead cell stain fluorescing at 568nm, in Phenol Red-Free culture medium for 30 minutes under low O_2 conditions before imaging. Imaging took place 24 hours after injury using the same BioRad 1024 Confocal Microscope. The same imaging parameters were utilized when imaging for viability as was used for imaging DHE except the 568nm wavelength was used to image EthD-2 instead of DHE.

3.5 Post-Impact Treatment

Explants were cultured for the same amount of time before impact as the pre-impact groups. Immediately after the impact, specimens were treated with either 20μM cytochalasin B (n=4) or 10μM nocodazole (n=5) in phenol red-free culture medium for four hours under low O_2 conditions. After four hours of treatment, specimens were placed in fresh, low O_2 equilibrated phenol red-free culture medium and incubated overnight under the previously used low O_2 conditions. Twenty-four hours after injury, specimens were imaged for viability using the same viability imaging protocol used for the pre-impact treatment and no treatment specimens.

3.6 Image Analysis

Confocal images were analyzed using ImageJ software (rsb.info.nih.gov/ij). For each site imaged, the raw01.pic file, corresponding to the DHE and EthD-2 stained specimens, was opened in ImageJ, and a threshold was applied. The threshold was established throughout the z-series stack so that cells stained in an image of the z-series stack were not counted in either its superior or inferior images. Specimens stained with DHE tended to have more background than those stained with EthD-2, so care was taken to not count background as DHE positive cells. Any DHE or EthD-2 stained cells of any shape and a size of 10 μm^2 or larger were counted by ImageJ and recorded for each site. Next, the raw02.pic file for the corresponding raw01.pic file was opened to analyze the Calcein AM stained, living chondrocytes at specific sites. Again, the z-series stack was thresholded so that cells were not counted more than once throughout the stack. Also, cells that were out of the plane of focus were not counted. The same size and shape parameters were used for counting Calcein AM stained cells as DHE and EthD-2 stained cells. For each site imaged, the number of Calcein AM stained cells was recorded.

To calculate the percent of DHE, ROS production, staining, the number of DHE positive cells was divided by the number of DHE positive cells plus the number of Calcein AM stained cells (Equation 1).

$$\%\ \text{DHE staining} = \frac{\text{DHE positive cells}}{(\text{DHE positive cells} + \text{Calcein AM positive cells})} \times 100 \quad (1)$$

To calculate the viability of chondrocytes 24 hours after injury, the number and Calcein AM stained cells were divided by the EthD-2 stained cells plus the Calcein AM stained cells (Equation 2).

$$\%\ \text{Viable} = \frac{\text{Calcein AM positive cells}}{(\text{Calcein AM positive cells} + \text{EthD}-2\ \text{positive cells})} \times 100 \quad (2)$$

3.7 Statistical Analysis

ROS production and viability data were pooled for the impact and control sites within the respective experimental groups. Kruskal-Wallis One Way ANOVAs on Ranks with either Dunn's method or Holm-Sidak method for post hoc testing were used to evaluate the effects on control and impact sites of experimental treatments on ROS production in pre-impact groups and on viability in pre- and post-impact groups.

3.8 Phalloidin Staining and Imaging

Medial, tibial plateau osteochondral explants were cultured as previously described for the lateral tibial plateaus. Explants were treated with either 20μM cytochalasin B or 10μM nocodazole for four hours or left untreated. At the end of the treatment, eight millimeter diameter semicircular, full-thickness cartilage sections were cryo-imbedded with tissue freezing medium (TFM; Triangle Biomedical Sciences, Inc.). Specimens were placed in a -80°C freezer overnight. Ten micrometer sections were then cut for each of the treatment groups and placed in a 4°C refrigerator overnight. The following day, the cut sections were taken out of the refrigerator and placed at room temperature for 20-30 minutes. Sections were fixed in 4% paraformaldehyde, 0.1% Triton-X-100 in 1x phosphate buffered saline (PBS) for five minutes. They were then wash twice with 1x PBS. The f-actin filaments were then stained with alexa fluor 488

phalloidin, obtained from the University of Iowa's Central Microscopy Research Facility, at a 1:40 dilution, 1% bovine serum albumin (BSA) in 1x PBS for 30 minutes at 37°C. Vectashield with DAPI (4', 6-diamidino-2-phenylindole; Vector Laboratories) was applied to the sections and covered with a coverslip.

Images of the three treatment groups were taken using a Zeiss 710 confocal microscope. Images at 20x and 63x were taken to get a general overview of the efficacy of the treatment groups and the effects of the treatments.

3.9 Overview

A generalized overview of the experimental setup is shown below (Figure 15). Lateral tibial plateaus were utilized for impact while medial explants were employed for looking at cytoskeletal responses to the different cytoskeletal inhibitors.

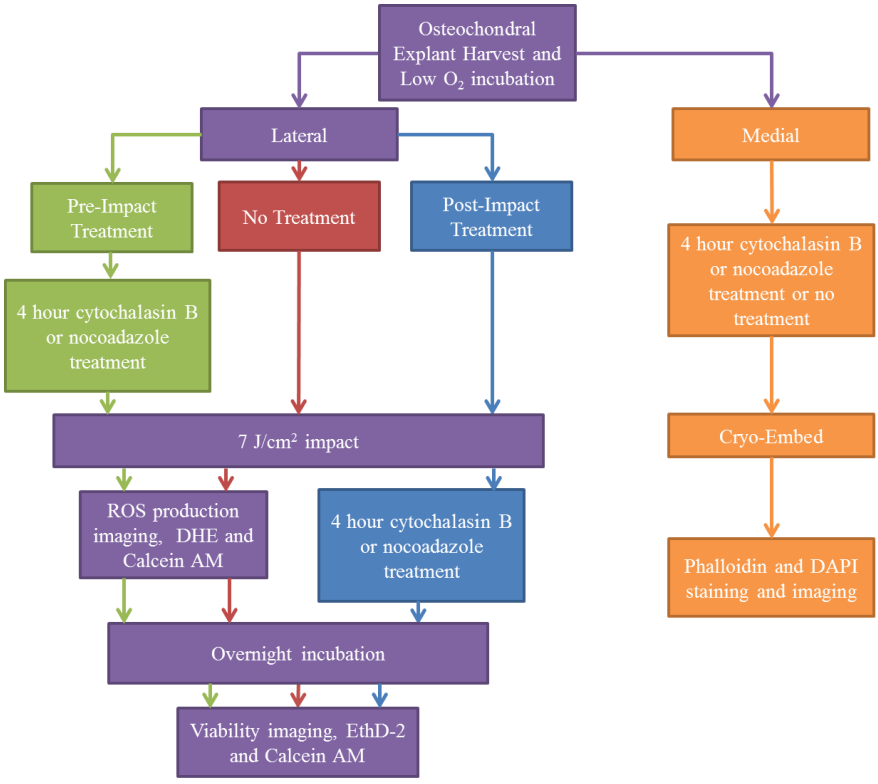

Figure 15. Flow chart of experimental procedures.

CHAPTER 4

RESULTS

4.1 Confocal Images

The effects of pre- and post-impact dissolution of the cytoskeletons of articular cartilage chondrocytes on reactive oxygen species (ROS) production and cell viability were studied using confocal microscopy. Confocal images taken directly after impact of DHE and Calcein AM stained chondrocytes of pre-impact treated osteochondral explants were analyzed for ROS production using ImageJ (Figure 16). Viability confocal images, using ethidium homodimer-2 and Calcein AM probes, of pre- and post-impact treated specimens 24 hours after impact were also analyzed using ImageJ. Overall, DHE stained

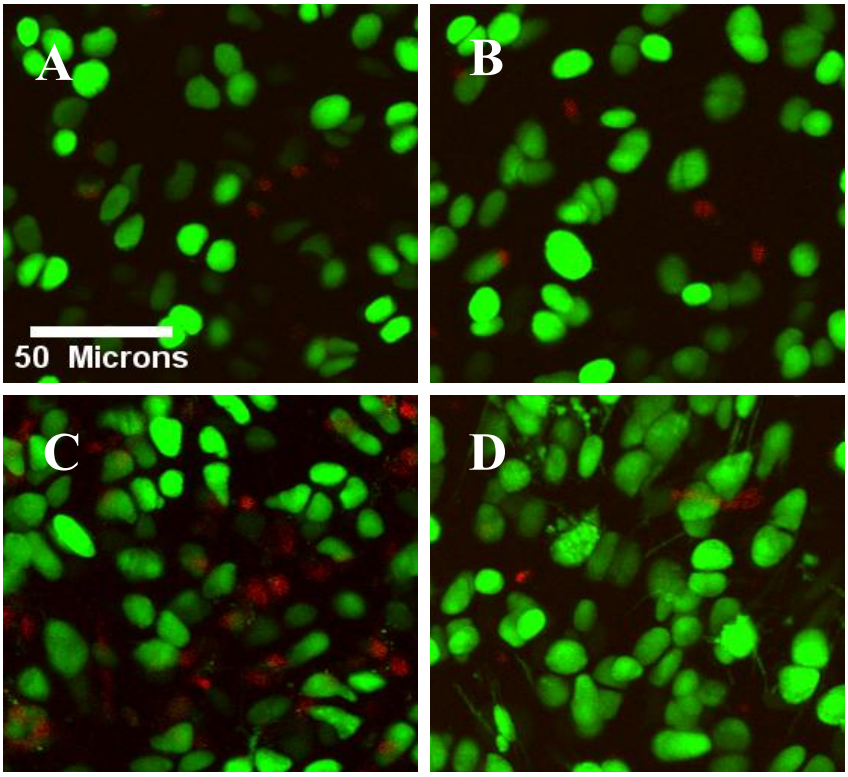

Figure 16. Z-series confocal images of DHE and Calcein AM stained chondrocytes. Representative images of A) impact sites of cytochalasin B treated specimens, B) impact sites of nocodazole treated specimens, C) impact sites of untreated specimens, and D) control sites of untreated specimens are shown. DHE is prevalent in the impact sites of untreated specimens than any of the other groups.

chondrocytes were more evident in the impact sites of untreated specimens than in the impact sites of the two pre-impact treatment groups (Figure 16). DHE staining in control sites was low across all specimens. Post-impact treated specimens were not able to be imaged directly after impact for ROS production because the four hour post-impact treatment was started directly after impact. Viability in impact sites of specimens treated with cytoskeletal inhibitors was shown to be greater than those of untreated specimens for both the pre- and post- impact treated specimens (Figure 17, Figure 18).

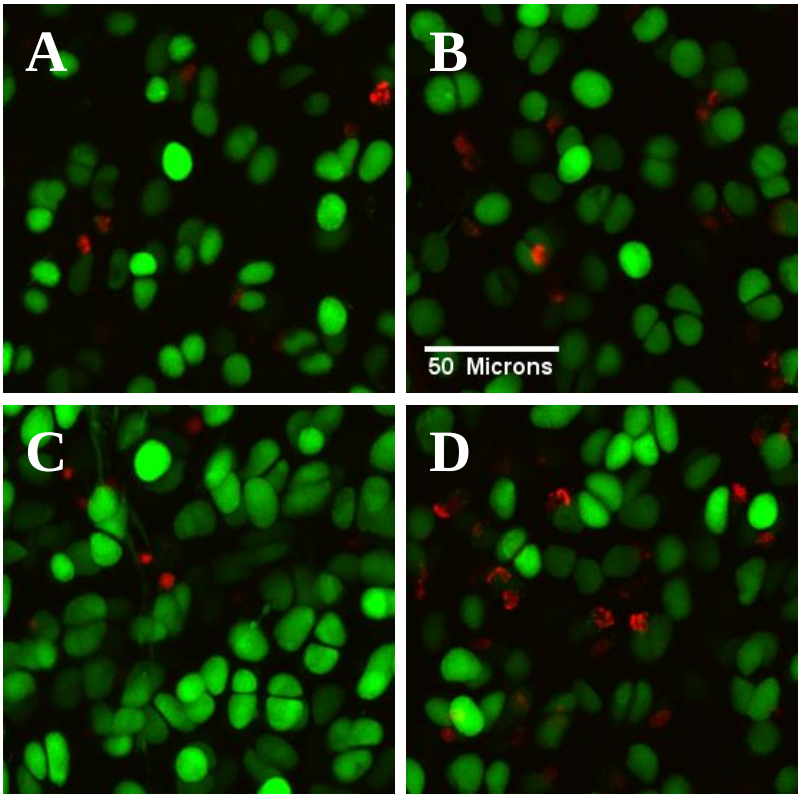

Figure 17. Viability of Z-series confocal images of EthD-2, red staining of the nucleus, and Calcein AM, green staining of the cytoplasm, stained chondrocytes. Representative images of the impact site of A) pre-impact treatment and B) post-impact treatment specimens, and C) the control site of untreated specimens and D) the impact site of untreated specimens. The scale bar is 50 microns and is equivalent for each image.

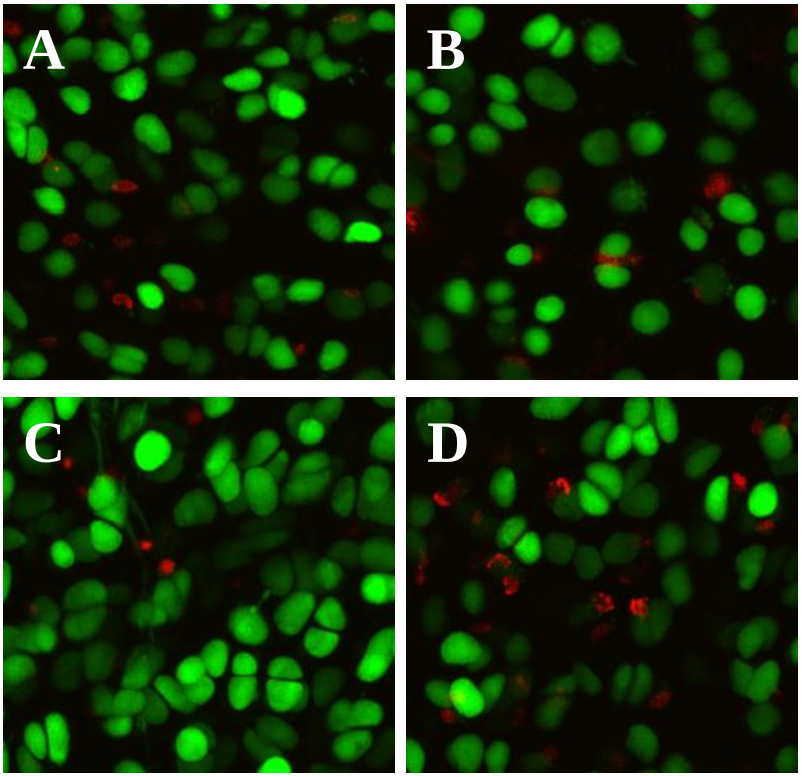

Figure 18. Viability of Z-series confocal images of EthD-2, red staining of the nucleus, and Calcein AM, green staining of the cytoplasm, stained chondrocytes. Representative images of A) the impact site of specimens pretreated with nocodazole, B) the impact site of delayed nocodazole treatment specimens, C) the control site of untreated specimens and D) the impact site of untreated specimens. The 50 micron scale bar in Figure 17 is representative of the scale of these images.

4.2 ROS Production after Impact

The effect of four hour pre-impact treatment with cytoskeletal inhibitors on ROS production was investigated directly after a 7 J/cm^2 injury (Figure 19). After blunt impact to articular cartilage, chondrocytes in the area that experienced impact loading produced more ROS than chondrocytes further away from the impact site in all treatment groups. No significant difference was seen between any of the control site groups of the different

treatment groups, and in general, DHE staining was lower at control sites than impact sites. However, when control data was pooled and compared with the ROS production of each treatment's impact sites, the only significant difference between control and impact groups was within in the untreated group, suggesting that treatment with either cytoskeletal inhibitor reduced DHE staining. Inhibition of chondrocytes' cytoskeletons reduced ROS production in damaged cartilage after blunt impact when compared with osteochondral explants that were left untreated (Figure 19). Specimens that were not treated with cytoskeletal inhibitors showed the highest DHE staining with 42.4% of

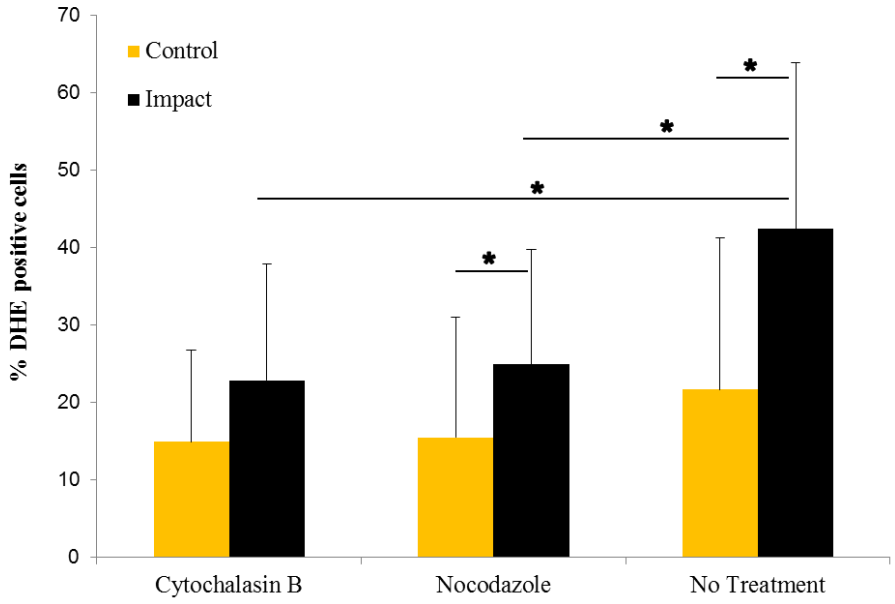

Figure 19. ROS production in impact and control sites of pre-impact treated and no treatment experimental groups.

chondrocytes within the impact zone producing ROS while cytochalasin B and nocodazole both significantly reduced ROS production ($p \leq 0.001$). Cytochalasin B reduced ROS production in impact sites by 19.5% (22.8% ROS production by impact zone chondrocytes) whereas nocodazole reduced it by 17.5% (24.9% ROS production).

Within treatment groups, explants treated with cytochalasin B were the only ones to show no significant difference between impact (22.8% DHE staining) and control sites (15.0% DHE staining) (p=0.05). Both the nocodazole treatment and no treatment experimental groups showed significant difference between impact sites and their respective control sites (15.5% to 24.9% for nocodazole and 21.7% to 42.4 for no treatment) (p=0.027 for nocodazole and p=0.002 for no treatment); however, DHE staining was lower in the impact sites of nocodazole treated specimens.

4.3 Viability 24 Hours after Impact

Chondrocyte viability was examined 24 hours after blunt impact using confocal microscopy for all pre- and post-impact experimental groups (Figure 20). Chondrocyte viability was greatest in the control sites for all experimental groups. Viability did not

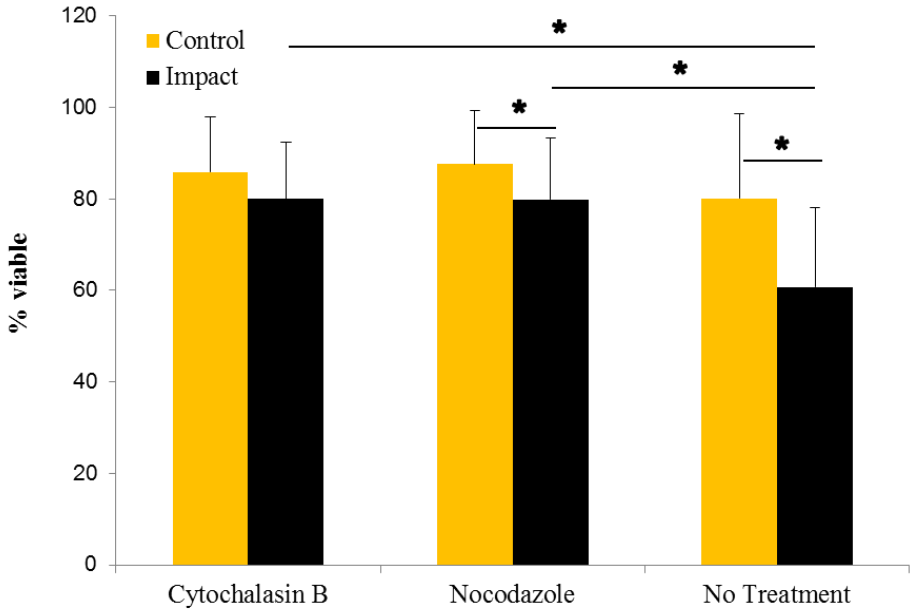

Figure 20. Viabilities of pre-impact treated and no treatment experimental groups 24 hours after impact.

differ in control sites ($p=0.387$ between pre-impact control sites and $p=0.303$ between post-impact control sites) suggesting that treatments were neither beneficial nor detrimental to articular cartilage health. To further support this finding, viabilities in the impact sites of cytochalasin B and nocodazole pre-impact treated specimens were not significantly different ($p=0.970$). Dissolution of chondrocytes' cytoskeletons prior to blunt impact reduced ROS production just after impact and increased chondrocyte viability 24 hours after injury in comparison to untreated specimens. When compared with the impact sites of the untreated experimental group (60.8% viability), viability in the impact sites of cytochalasin B treated specimens, 80.0% viable, was 19.3% higher than untreated specimens, and the impact sites of nocodazole treated specimens, 79.9% viable, was 19.1% higher than untreated specimens (Figure 20). These viabilities in impact sites of the two pre-impact groups treated with cytoskeletal inhibitors are significantly greater than that of the untreated group ($p<0.001$). Although pre-impact treatment with either cytochalasin B or nocodazole greatly improved chondrocyte viability 24 hours after impact, neither was superior to the other in saving chondrocytes ($p=0.970$). However, the impact and control sites of cytochalasin B treated explants showed no significant difference in viability ($p=0.073$), whereas corresponding impact and control sites of both the pre-impact nocodazole treated and untreated specimens varied significantly, $p=0.017$ and $p=0.004$, respectively.

Viabilities of the post-impact cytochalasin B and nocodazole treatment groups were similar to those of the pre-impact experimental groups. However, the viabilities in the impact sites were slightly lower than in the pre-impact treatment groups (75.6% post-impact viability compared with 80.0% for pre-impact specimens treated with cytochalasin B and 75.9% post-impact to 79.9% pre-impact for nocodazole treated specimens), though these differences were not significant (Figure 21).

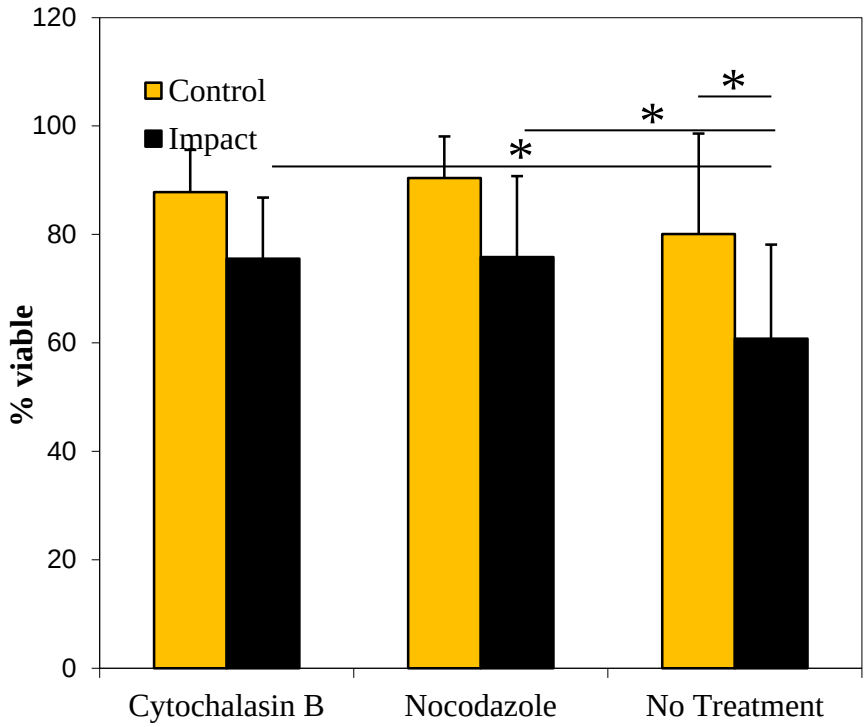

Figure 21. Viabilities of post-impact treated and no treatment experimental groups 24 hours after impact.

4.4 Phalloidin Staining of the F-actin

To determine the effects of cytoskeletal inhibitors on the organization of f-actin in articular cartilage, specimens treated with cytochalasin B, nocodazole, or left untreated were and stained with phalloidin, which stains the f-actin of cells. Confocal images of phalloidin and DAPI stained articular cartilage showed a lack staining of f-actin in chondrocytes in the superficial zone after four hour treatment in both the cytochalasin B and the nocodazole treated groups. However, a cortical f-actin network is visible throughout the entire thickness of untreated specimens (Figure 22).

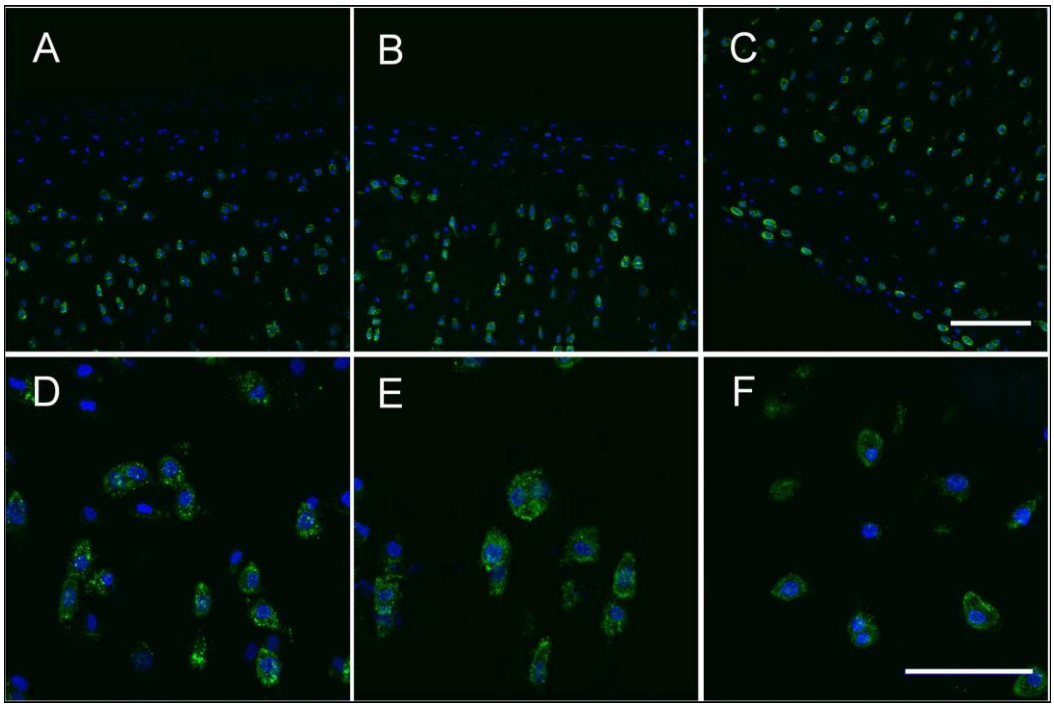

Figure 22. Phalloidin staining (green) and DAPI staining (blue) of sagittal sections of A) and D) cytochalasin B treated, B) and E) nocodazole treated, and C) and F) no treatement specimens. Scale bars represent 100μm for the top row of images and 50μm for the bottom row of images.

CHAPTER 5

DISCUSSION

The results of these experiments demonstrated that the dissolution of chondrocytes' cytoskeletons prior to and after impact injury significantly reduced reactive oxygen species (ROS) production and chondrocyte death following impact injury. The acute release of excessive ROS after injury seems to be linked to chondrocyte death following impact injury as shown by Martin et al.[7] In these experiments, not only was ROS production reduced by inhibiting the chondrocyte cytoskeleton, but chondrocyte viability was also higher in those specimens that released less ROS than those that released greater amounts of ROS. Studies have shown that mechanical stresses instigate the release of ROS, not only during injurious loading but under regular dynamic loading.[8, 53] This implies that not all ROS are harmful to cartilage, but some production is vital to the maintenance of homeostasis. However, in large amounts, such as after an injury, ROS have adverse effects on cartilage. Scavenging of ROS with antioxidants after an impact injury has been shown to reduce impact related chondrocyte death which indicates that ROS as the culprit causing chondrocyte death.[7] Goodwin et al. were able to show that this detrimental release of ROS following impact injury is mitochondrial in origin and can be mitigated by inhibiting electron transfer in complex I of the mitochondrial electron transport chain.[8] Together with the current experiments, these results suggest that the inhibition of the cytoskeletal elements of chondrocytes prevented mitochondrial release of injurious amounts of ROS, saving chondrocytes following injury. Also, they show that mitochondria play an important role in the mechanobiologic signaling pathways in articular cartilage in conjunction with the chondrocyte cytoskeleton.

The chondrocyte cytoskeleton executes many functions. It aids in the structural integrity of the chondrocyte and the mechanotransduction of different intracellular signals, to name a few. Microfilaments, in particular filamentous actin or f-actin, are

responsible for the resistance to compression of the chondrocyte cytoskeleton.[40] Dissolution of the microfilament network in leads to the greatest decline in chondrocyte stiffness when compared with the dissolution of any of the other cytoskeletal elements. Microfilaments have been shown to be more densely situated in the chondrocytes of the superficial zone and in general, are concentrated around the periphery of chondrocytes, securing chondrocytes to the surrounding matrix by associations with integrin proteins[11]. This link between chondrocytes and their extracellular matrix (ECM) allows for the mechanotransduction of tissue level strains in articular cartilage to the chondrocyte and its intracellular organelles, including the mitochondria. Mitochondria are attached to the microfilaments throughout the cell which allows them to be transported across the cell to areas of high energy consumption. The microtubule network is also associated with the mitochondria and plays a role in cell recovery after loading. Dissolution of the microfilaments by cytochalasin D or the microtubules by nocodazole leads to the decreased cellular motion of mitochondria.[51] It has also been shown that under an applied load, mitochondria deform because of their connection to the cytoskeleton, and with inhibition of the cytoskeleton, mitochondria do not experience significant deformation upon loading.[10] This evidence strongly implies that mechanical strains applied to the surface of articular cartilage are conveyed to and deform the mitochondria by means of the chondrocyte cytoskeleton. Therefore, it is plausible that inhibition of these cytoskeletal elements disconnected the mitochondria from the cytoskeleton, preventing pathologic strains due to impact injury to deform chondrocyte mitochondria and release ROS which parallels the results of these experiments. In turn, the decrease in mitochondrial release of ROS lead to greater chondrocyte viability 24 hours after impact signifying a relationship between excessive ROS release, cell death, and the chondrocyte cytoskeleton. However, it is possible that some other unknown mechanism affects intracellular ROS release other than mitochondrial deformation.

Not only was viability 24 hours after impact improved by treatment with cytoskeletal inhibitors prior to impact injury, but it was also enhanced with post-impact treatments. This suggests that the dissolution of the cytoskeleton after injury possibly relieves residual strain on the chondrocytes and mitochondria from the injury. Increased viability after delayed treatment with cytoskeletal elements indicates that there could be window of opportunity for treatment of cartilage injuries with cytoskeletal inhibitors. However, both drugs used in this experiment are toxic, so a different treatment would need to be used.

The dissolution of the chondrocyte cytoskeleton was verified in confocal images of osteochondral explants treated with either cytochalasin B or nocodazole. Even though nocodazole depolymerizes microtubules and not f-actin, the dissociation of the f-actin network was apparent in confocal images of the phalloidin stained explant treated with nocodazole. Dissociation of just one of the cytoskeletal elements essential to the tensegrity of the cell compromises the entire structural integrity of the chondrocyte.[39] Therefore, dissociation of the microfilament network by a microtubule inhibitor should be expected. Confocal images clearly show a definite boundary between intact and fragmented microfilament networks in the two explants treated with either cytochalasin B or nocodazole when compared with which may be a result of the penetration of the drug into the explant which could be inhibited by the presence of large amount of proteoglycans. The perceptible depth of penetration of the drugs corresponded with the superficial zone of articular cartilage which paralleled the depth of the confocal images of impacted cartilage taken to investigate ROS production and viability.

Confocal images of osteochondral explants taken with the BioRad 1024 Confocal Microscope effectively showed the superficial 150 to 200 micrometers, but could not image chondrocytes deeper in the cartilage, limiting analyses to the superficial and upper transitional zone. However, it has been shown that the majority of cell death after injury occurs in the superficial cartilage zone and adjacent to cracks; therefore, analyses of the

confocal images likely represent the chondrocytes most affected by injury.[5] Since chondrocyte density within and across specimens varies enough that it can obscure experimental analyses, an x-y imaging table and plastic imaging plates were used to ensure that images for ROS and viability were taken in the same site. The x-y imaging table allows for 10 micrometers of leeway.

These experiments only studied the effects of treatments directly and 24 hours after articular cartilage injury. Other studies have shown that apoptotic chondrocyte death starts one to two days after injury and can develop over seven to fourteen days. Therefore, the long term effects of cytochalasin B and nocodazole treatment on chondrocyte viability are unknown. It is possible that these drugs had a more direct effect on mitochondrial function than the cytoskeleton. Also, alternative sources of ROS, other than ones that are mitochondrial in origin, were not included in this study. However, previous studies have established that injury related ROS production was produced by the mitochondria, so it is reasonable to assume that the ROS produced upon cartilage injury originates in the mitochondria.

In conclusion, articular cartilage treated with agents that inhibit the polymerization of cytoskeletal elements prior to impact significantly decreased the amount of ROS produced after an impact injury. Twenty-four hours following impact injury, the chondrocytes of all the treated experimental groups had greater viability than explants that were left untreated. It is likely that the dissolution of the microfilaments and microtubules prior to and after impact injury reduced impact-related chondrocyte death by reducing the mitochondrial ROS production. Strain from the impact could not be transmitted to the mitochondria because the association between the mitochondria and cytoskeleton had been compromised. These findings support further investigation into the mechanotransduction of cellular signaling upon articular cartilage injury which could advance the understanding of the progression of PTOA and help to develop treatment strategies to prevent PTOA.

APPENDIX

Table A1. Raw counts of DHE and Calcein AM staining of cytochalasin B pre-impact treated explants directly after 7 J/cm^2 impact injury.

	Control			Impact		
Explant	**DHE positive cells**	**Calcein AM**	**% DHE**	**DHE poitive cells**	**Calcein AM**	**% DHE**
1288R	0	165	0.000	25	80	23.810
	0	151	0.000	23	87	20.909
	0	125	0.000	21	96	17.949
1294L	29	184	13.615	3	107	2.727
	5	192	2.538	4	124	3.125
	29	144	16.763	8	82	8.889
1301R	108	228	32.143	151	118	56.134
	69	184	27.273	59	96	38.065
	87	155	35.950	75	110	40.541
1302L	27	102	20.930	22	138	13.750
	61	143	29.902	28	124	18.421
	24	99	19.512	41	92	30.827
1309L	62	185	25.101	61	226	21.254
	80	200	28.571	129	114	53.086
	50	317	13.624	81	177	31.395
1310R	94	313	23.096	212	346	37.993
	76	238	24.204	102	271	27.346
	62	372	14.286	102	195	34.343
1443R	2	348	0.571	48	215	18.251
	1	195	0.510	59	192	23.506
	68	301	18.428	31	206	13.080
1444R	2	178	1.111	14	278	4.795
	23	318	6.745	9	220	3.930
	13	319	3.916	13	250	4.943

Table A2. Raw counts of EthD-2 and Calcein AM staining of cytochalasin B pre-impact treated explants 24 hours after 7 J/cm^2 impact injury.

	Control			Impact		
Explant	**EthD-2**	**Calcein AM**	**% Viable**	**EthD-2**	**Calcein AM**	**% Viable**
1288R	22	252	91.971	8	184	95.833
	10	177	94.652	16	172	91.489
	8	108	93.103	4	221	98.222
1294L	9	203	95.755	33	122	78.710
	61	118	65.922	76	117	60.622
	71	150	67.873	14	123	89.781
1301R	72	230	76.159	38	69	64.486
	64	95	59.748	31	66	68.041
	32	98	75.385	57	81	58.696
1302L	46	143	75.661	28	140	83.333
	12	192	94.118	39	98	71.533
	35	120	77.419	35	83	70.339
1309L	6	171	96.610	44	176	80.000
	5	150	96.774	11	126	91.971
	5	250	98.039	110	165	60.000
1310R	18	197	91.628	77	254	76.737
	87	188	68.364	68	238	77.778
	82	273	76.901	81	165	67.073
1443R	5	247	98.016	41	244	85.614
	9	119	92.969	6	113	94.958
	10	198	95.192	14	172	92.473
1444R	7	154	95.652	33	235	87.687
	36	273	88.350	34	181	84.186
	18	336	94.915	21	228	91.566

Table A3. Raw counts of DHE and Calcein AM staining of nocodazole pre-impact treated explants directly after 7 J/cm^2 impact injury.

	Control			Impact		
Explant	**DHE positive cells**	**Calcein AM**	**% DHE**	**DHE positive cells**	**Calcein AM**	**% DHE**
1343L	2	248	0.800	27	325	7.670
	2	198	1.000	34	204	14.286
	1	262	0.380	35	244	12.545
1344?	1	114	0.870	3	194	1.523
	1	115	0.862	55	201	21.484
	0	119	0.000	14	222	5.932
1360L	51	217	19.030	88	210	29.530
	24	131	15.484	62	172	26.496
	5	294	1.672	70	110	38.889
1419R	30	115	20.690	36	111	24.490
	75	144	34.247	46	93	33.094
	34	182	15.741	18	102	15.000
1427R	83	168	33.068	58	181	24.268
	48	102	32.000	86	117	42.365
	124	184	40.260	98	80	55.056
1434L	115	324	26.196	176	162	52.071
	107	83	56.316	154	234	39.691
	27	195	12.162	126	189	40.000
1451L	55	144	27.638	32	136	19.048
	38	193	16.450	68	148	31.481
	10	139	6.711	32	234	12.030
1454R	9	180	4.762	44	89	33.083
	5	198	2.463	9	115	7.258
	4	151	2.581	10	80	11.111

Table A4. Raw counts of EthD-2 and Calcein AM staining of nocodazole pre-impact treated explants 24 hours after 7 J/cm^2 impact injury.

	Control			Impact		
Explant	**EthD-2**	**Calcein AM**	**% Viable**	**EthD-2**	**Calcein AM**	**% Viable**
1343L	2	235	99.156	22	158	87.778
	5	207	97.642	6	211	97.235
	6	218	97.321	8	220	96.491
1344?	1	152	99.346	5	202	97.585
	3	136	97.842	71	200	73.801
	2	155	98.726	15	248	94.297
1360L	5	222	97.797	68	186	73.228
	40	80	66.667	62	190	75.397
	19	191	90.952	85	207	70.890
1419R	17	116	87.218	33	112	77.241
	50	148	74.747	23	84	78.505
	30	131	81.366	18	52	74.286
1427R	55	129	70.109	100	123	55.157
	80	115		99	85	
	60	152	71.698	69	127	64.796
1434L	93	191		24	67	73.626
	17	84	83.168	72	123	63.077
	16	93	85.321	138	85	
1451L	39	75	65.789	48	90	65.217
	13	89	87.255	47	90	65.693
	11	59	84.286	27	128	82.581
1454R	4	179	97.814	5	133	96.377
	3	134	97.810	3	121	97.581
	4	117	96.694	3	87	96.667

Table A5. Raw counts of DHE and Calcein AM staining of untreated explants directly after 7 J/cm^2 impact injury.

	Control			Impact		
Explant	**DHE positive cells**	**Calcein AM**	**% DHE**	**DHE positive cells**	**Calcein AM**	**% DHE**
1425R	176	108	61.972	262	68	79.394
	106	190	35.811	200	42	82.645
	125	115	52.083	180	83	68.441
1465R	5	330	1.493	100	238	29.586
	10	283	3.413	87	211	29.195
	4	288	1.370	105	280	27.273
1469R	172	383	30.991	126	78	61.765
	107	120	47.137	30	44	40.541
	63	84	42.857	81	72	52.941
1470R	46	321	12.534	106	119	47.111
	10	215	4.444	50	133	27.322
	0	321	0.000	71	214	24.912
1484R	90	341	20.882	78	107	42.162
	54	253	17.590	220	172	56.122
	9	165	5.172	189	122	60.772
1628R	85	248	25.526	176	301	36.897
	11	363	2.941	128	254	33.508
	30	257	10.453	202	142	58.721
1630R	197	250	44.072	29	319	8.333
	105	233	31.065	28	316	8.140
	10	326	2.976	51	287	15.089

Table A6. Raw counts of EthD-2 and Calcein AM staining of untreated explants 24 hours after 7 J/cm^2 impact injury.

	Control			Impact		
Explant	**EthD-2**	**Calcein AM**	**% Viable**	**EthD-2**	**Calcein AM**	**% Viable**
1425R	54	122	69.318	56	63	52.941
	140	97	40.928	122	22	15.278
	55	68	55.285	73	64	46.715
1465R	3	307	99.032	85	207	70.890
	30	228	88.372	70	217	75.610
	14	322	95.833	84	208	71.233
1469R	36	188	83.929	111	61	35.465
	80	89	52.663	37	44	54.321
	2	71	97.260	30	43	58.904
1470R	58	131	69.312	67	124	64.921
	4	145	97.315	38	88	69.841
	3	319	99.068	78	227	74.426
1484R	32	214	86.992	30	160	84.211
	63	205	76.493	87	132	60.274
	4	167	97.661	55	111	66.867
1628R	179	210	53.985	153	171	52.778
	41	293	87.725	107	264	71.159
	54	155	74.163	205	156	43.213
1630R	110	196		25	230	
	112	195		39	256	
	14	373	96.382	34	203	85.654

Table A7. Raw counts of EthD-2 and Calcein AM staining of cytochalasin B post-impact treated explants 24 hours after 7 J/cm^2 impact injury.

	Control			Impact		
Explant	**EthD-2**	**Calcein AM**	**% Viable**	**EthD-2**	**Calcein AM**	**% Viable**
1535R	19	156	89.143	47	125	72.674
	29	162	84.817	46	136	74.725
	35	251	87.762	42	121	74.233
1538L	43	282	86.769	22	228	91.200
	10	184	94.845	51	159	75.714
	12	104	89.655	59	177	75.000
1545L	21	199	90.455	73	133	64.563
	3	183	98.387	102	133	56.596
	16	109	87.200	79	127	61.650
1555L	48	97	66.897	12	131	91.608
	18	257	93.455	41	158	79.397
	52	275	84.098	21	177	89.394

Table A8. Raw counts of EthD-2 and Calcein AM staining of nocodazole post-impact treated explants 24 hours after 7 J/cm^2 impact injury.

	Control			Impact		
Explant	**EthD-2**	**Calcein AM**	**% Viable**	**EthD-2**	**Calcein AM**	**% Viable**
1567R	8	172	95.556	21	161	88.462
	35	193	84.649	36	200	84.746
	1	172	99.422	12	244	95.313
1569R	3	220	98.655	58	129	68.984
	56	209	78.868	36	211	85.425
	25	128	83.660	46	166	78.302
1574R	50	180	78.261	136	159	53.898
	3	314	99.054	86	126	59.434
	40	181	81.900	145	147	50.342
1575L	8	341	97.708	36	210	85.366
	6	329	98.209	26	253	90.681
	45	325	87.838	47	173	78.636
1579L	33	316	90.544	160	235	59.494
	13	206	94.064	109	217	66.564
	33	240	87.912	30	354	92.188

REFERENCES

1. Kiani, C., et al., *Structure and function of aggrecan.* Cell Research, 2002. **12**(1): p. 19-32.

2. Van Raamsdonk, J.M. and S. Hekimi, *Reactive Oxygen Species and Aging in Caenorhabditis elegans: Causal or Casual Relationship?* Antioxid Redox Signal, 2010. **13**(12): p. 1911-53.

3. Davisson, T., et al., *Static and dynamic compression modulate matrix metabolism in tissue engineered cartilage.* Journal of Orthopaedic Research, 2002. **20**(4): p. 842-8.

4. Andriacchi, T.P., S. Koo, and S.F. Scanlan, *Gait mechanics influence healthy cartilage morphology and osteoarthritis of the knee.* Journal of Bone and Joint Surgery, 2009. **91 Suppl 1**: p. 95-101.

5. D'Lima, D.D., et al., *Human chondrocyte apoptosis in response to mechanical injury.* Osteoarthritis and Cartilage, 2001. **9**(8): p. 712-9.

6. Chen, A.F., et al., *Oxidative DNA damage in osteoarthritic porcine articular cartilage.* Journal of Cellular Physiology, 2008. **217**(3): p. 828-33.

7. Martin, J.A., et al., *N-acetylcysteine inhibits post-impact chondrocyte death in osteochondral explants.* Journal of Bone and Joint Surgery, 2009. **91**(8): p. 1890-7.

8. Goodwin, W., et al., *Rotenone prevents impact-induced chondrocyte death.* Journal of Orthopaedic Research, 2010. **28**(8): p. 1057-63.

9. Guilak, F., A. Ratcliffe, and V.C. Mow, *Chondrocyte deformation and local tissue strain in articular cartilage: a confocal microscopy study.* Journal of Orthopaedic Research, 1995. **13**(3): p. 410-21.

10. Knight, M.M., et al., *Chondrocyte deformation induces mitochondrial distortion and heterogeneous intracellular strain fields.* Biomech Model Mechanobiol, 2006. **5**(2-3): p. 180-91.

11. Langelier, E., et al., *The chondrocyte cytoskeleton in mature articular cartilage: structure and distribution of actin, tubulin, and vimentin filaments.* Journal of Histochemistry and Cytochemistry, 2000. **48**(10): p. 1307-20.

12. Brown, T.D., et al., *Posttraumatic osteoarthritis: a first estimate of incidence, prevalence, and burden of disease.* Journal of Orthopaedic Trauma, 2006. **20**(10): p. 739-44.

13. Blanco, F.J., I. Rego, and C. Ruiz-Romero, *The role of mitochondria in osteoarthritis.* Nat Rev Rheumatol, 2011. **7**(3): p. 161-9.

14. McKinley, T.O., et al., *Basic science of intra-articular fractures and posttraumatic osteoarthritis.* Journal of Orthopaedic Trauma, 2010. **24**(9): p. 567-70.

15. Laird, A. and J.F. Keating, *Acetabular fractures: a 16-year prospective epidemiological study.* Journal of Bone and Joint Surgery. British Volume, 2005. **87**(7): p. 969-73.

16. Dirschl, D.R., et al., *Articular fractures.* Journal of the American Academy of Orthopaedic Surgeons, 2004. **12**(6): p. 416-23.

17. Marsh, J.L., D.P. Weigel, and D.R. Dirschl, *Tibial plafond fractures. How do these ankles function over time?* Journal of Bone and Joint Surgery, 2003. **85-A**(2): p. 287-95.

18. Anderson, D.D., et al., *Post-traumatic osteoarthritis: Improved understanding and opportunities for early intervention.* Journal of Orthopaedic Research, 2011. **29**(6): p. 802-9.

19. Moore, K.L., A.F. Dalley, and A.M.R. Agur, *Clinically oriented anatomy*. 5th ed. 2006, Philadelphia: Lippincott Williams & Wilkins. xxxiii, 1209 p.

20. Hoshino, A. and W.A. Wallace, *Impact-absorbing properties of the human knee.* Journal of Bone and Joint Surgery. British Volume, 1987. **69**(5): p. 807-11.

21. Bhosale, A.M. and J.B. Richardson, *Articular cartilage: structure, injuries and review of management.* British Medical Bulletin, 2008. **87**: p. 77-95.

22. Shirazi, R., A. Shirazi-Adl, and M. Hurtig, *Role of cartilage collagen fibrils networks in knee joint biomechanics under compression.* Journal of Biomechanics, 2008. **41**(16): p. 3340-8.

23. Buckwalter, J.A. and J.A. Martin, *Sports and osteoarthritis.* Current Opinion in Rheumatology, 2004. **16**(5): p. 634-9.

24. Brandt, K.D., *Response of joint structures to inactivity and to reloading after immobilization.* Arthritis and Rheumatism, 2003. **49**(2): p. 267-71.

25. Holtzer, H., et al., *The Loss of Phenotypic Traits by Differentiated Cells in Vitro, I. Dedifferentiation of Cartilage Cells.* Proceedings of the National Academy of Sciences of the United States of America, 1960. **46**(12): p. 1533-42.

26. Wei, F., et al., *Effect of intermittent cyclic preloads on the response of articular cartilage explants to an excessive level of unconfined compression.* Journal of Orthopaedic Research, 2008. **26**(12): p. 1636-42.

27. Szafranski, J.D., et al., *Chondrocyte mechanotransduction: effects of compression on deformation of intracellular organelles and relevance to cellular biosynthesis.* Osteoarthritis and Cartilage, 2004. **12**(12): p. 937-46.

28. Ohashi, T., et al., *Intracellular mechanics and mechanotransduction associated with chondrocyte deformation during pipette aspiration.* Biorheology, 2006. **43**(3-4): p. 201-14.

29. Tochigi, Y., et al., *Distribution and progression of chondrocyte damage in a whole-organ model of human ankle intra-articular fracture.* Journal of Bone and Joint Surgery, 2011. **93**(6): p. 533-9.

30. Loening, A.M., et al., *Injurious mechanical compression of bovine articular cartilage induces chondrocyte apoptosis.* Archives of Biochemistry and Biophysics, 2000. **381**(2): p. 205-12.

31. D'Lima, D.D., et al., *Cartilage injury induces chondrocyte apoptosis.* Journal of Bone and Joint Surgery, 2001. **83-A Suppl 2**(Pt 1): p. 19-21.

32. D'Lima, D.D., et al., *Impact of mechanical trauma on matrix and cells.* Clin Orthop Relat Res, 2001(391 Suppl): p. S90-9.

33. Otsuki, S., et al., *The effect of glycosaminoglycan loss on chondrocyte viability: a study on porcine cartilage explants.* Arthritis and Rheumatism, 2008. **58**(4): p. 1076-85.

34. Chen, C.T., et al., *Chondrocyte necrosis and apoptosis in impact damaged articular cartilage.* Journal of Orthopaedic Research, 2001. **19**(4): p. 703-11.

35. Bush, P.G., et al., *Viability and volume of in situ bovine articular chondrocytes-changes following a single impact and effects of medium osmolarity.* Osteoarthritis and Cartilage, 2005. **13**(1): p. 54-65.

36. Walsh, D.A., et al., *Angiogenesis and nerve growth factor at the osteochondral junction in rheumatoid arthritis and osteoarthritis.* Rheumatology, 2010. **49**(10): p. 1852-61.

37. Ashraf, S. and D.A. Walsh, *Angiogenesis in osteoarthritis.* Current Opinion in Rheumatology, 2008. **20**(5): p. 573-80.

38. Becker, W.M., L.J. Kleinsmith, and J. Hardin, *The world of the cell*. 6th ed. 2005, San Francisco: Pearson Benjamin Cummings, Inc. xxvi, 795, 90 p.

39. Ingber, D.E., *Tensegrity-based mechanosensing from macro to micro.* Progress in Biophysics and Molecular Biology, 2008. **97**(2-3): p. 163-79.

40. Ofek, G., D.C. Wiltz, and K.A. Athanasiou, *Contribution of the cytoskeleton to the compressive properties and recovery behavior of single cells.* Biophysical Journal, 2009. **97**(7): p. 1873-82.

41. Krendel, M., G. Sgourdas, and E.M. Bonder, *Disassembly of actin filaments leads to increased rate and frequency of mitochondrial movement along microtubules.* Cell Motility and the Cytoskeleton, 1998. **40**(4): p. 368-78.

42. Parkkinen, J.J., et al., *Altered Golgi apparatus in hydrostatically loaded articular cartilage chondrocytes.* Annals of the Rheumatic Diseases, 1993. **52**(3): p. 192-8.

43. Jortikka, M.O., et al., *The role of microtubules in the regulation of proteoglycan synthesis in chondrocytes under hydrostatic pressure.* Archives of Biochemistry and Biophysics, 2000. **374**(2): p. 172-80.

44. Liu, S., et al., *Dynamic modulation of cytoskeleton during in vitro maturation in human oocytes.* American Journal of Obstetrics and Gynecology, 2010. **203**(2): p. 151 e1-7.

45. Rotsch, C. and M. Radmacher, *Drug-induced changes of cytoskeletal structure and mechanics in fibroblasts: an atomic force microscopy study.* Biophysical Journal, 2000. **78**(1): p. 520-35.

46. Durrant, L.A., et al., *Organisation of the chondrocyte cytoskeleton and its response to changing mechanical conditions in organ culture.* Journal of Anatomy, 1999. **194 (Pt 3)**: p. 343-53.

47. MacLean-Fletcher, S. and T.D. Pollard, *Mechanism of action of cytochalasin B on actin.* Cell, 1980. **20**(2): p. 329-41.

48. Bonder, E.M. and M.S. Mooseker, *Cytochalasin B slows but does not prevent monomer addition at the barbed end of the actin filament.* Journal of Cell Biology, 1986. **102**(1): p. 282-8.

49. Pollard, T.D. and M.S. Mooseker, *Direct measurement of actin polymerization rate constants by electron microscopy of actin filaments nucleated by isolated microvillus cores.* Journal of Cell Biology, 1981. **88**(3): p. 654-9.

50. Kim, J., et al., *Mitochondrial DNA damage is involved in apoptosis caused by pro-inflammatory cytokines in human OA chondrocytes.* Osteoarthritis and Cartilage, 2010. **18**(3): p. 424-32.

51. Silberberg, Y.R., et al., *Mitochondrial displacements in response to nanomechanical forces.* Journal of Molecular Recognition, 2008. **21**(1): p. 30-6.

52. Knowles, M.K., et al., *Cytoskeletal-assisted dynamics of the mitochondrial reticulum in living cells.* Proceedings of the National Academy of Sciences of the United States of America, 2002. **99**(23): p. 14772-7.

53. Ali, M.H., et al., *Mitochondrial requirement for endothelial responses to cyclic strain: implications for mechanotransduction.* Am J Physiol Lung Cell Mol Physiol, 2004. **287**(3): p. L486-96.

54. Lee, R.B. and J.P. Urban, *Functional replacement of oxygen by other oxidants in articular cartilage.* Arthritis and Rheumatism, 2002. **46**(12): p. 3190-200.

55. Ysart, G.E. and R.M. Mason, *Responses of articular cartilage explant cultures to different oxygen tensions.* Biochimica et Biophysica Acta, 1994. **1221**(1): p. 15-20.

56. Henrotin, Y.E., P. Bruckner, and J.P. Pujol, *The role of reactive oxygen species in homeostasis and degradation of cartilage.* Osteoarthritis and Cartilage, 2003. **11**(10): p. 747-55.

57. Fay, J., et al., *Reactive oxygen species induce expression of vascular endothelial growth factor in chondrocytes and human articular cartilage explants.* Arthritis Res Ther, 2006. **8**(6): p. R189.

58. Coyle, C.H., N.J. Izzo, and C.R. Chu, *Sustained hypoxia enhances chondrocyte matrix synthesis.* Journal of Orthopaedic Research, 2009. **27**(6): p. 793-9.

59. Beecher, B.R., et al., *Antioxidants block cyclic loading induced chondrocyte death.* Iowa Orthopaedic Journal, 2007. **27**: p. 1-8.